

**METHODS FOR REDUCED PLATEN COMPRESSION (RPC) TEST  
SPECIMEN CUTTING LOCATIONS USING MICRO-CT AND  
PLANAR RADIOGRAPHS**

A Thesis

by

HEBER LEMMON

Submitted to the Office of Graduate Studies of  
Texas A&M University  
in partial fulfillment of the requirements for the degree of

MASTER OF SCIENCE

August 2003

Major Subject: Mechanical Engineering

**METHODS FOR REDUCED PLATEN COMPRESSION (RPC) TEST  
SPECIMEN CUTTING LOCATIONS USING MICRO-CT AND  
PLANAR RADIOGRAPHS**

A Thesis

by

HEBER LEMMON

Submitted to Texas A&M University  
in partial fulfillment of the requirements  
for the degree of

MASTER OF SCIENCE

Approved as to style and content by:

---

Harry Hogan  
(Chair of Committee)

---

Susan Bloomfield  
(Member)

---

Terry Creasy  
(Member)

---

Dennis O'Neal  
(Head of Department)

August 2003

Major Subject: Mechanical Engineering

## ABSTRACT

Methods for Reduced Platen Compression (RPC) Test Specimen Cutting Locations  
Using Micro-CT and Planar Radiographs. (August 2003)

Heber Lemmon, B.S., University of Idaho

Chair of Advisory Committee: Dr. Harry Hogan

This study looks at improving reduced platen compression (RPC) specimen preparation procedures by developing a better method for locating the ideal RPC specimen on each bone. These improvements are aimed at decreasing the amount of time required to complete an RPC analysis and improving the quality of the obtained results. High-resolution micro-CT scans are used to gain a better understanding of rat long bone anatomy by quantifying the location, shape, and orientation of the growth plate, primary spongiosa, and secondary spongiosa.

Micro-CT analysis shows that there are easily identifiable external landmarks on the anterior side of both tibias and femurs that identify the end of the growth plate and the point at which the top of an ideal RPC specimen should be located. The landmarks are the most proximal tip of the patellar surface for the femur and the base of the tibial tuberosity for the tibia.

This study also analyzes the effect of variations in the actual RPC specimen location from the ideal location and the effect of different platen sizes on test results using BMD as a surrogate for mechanical properties. The analysis shows that the BMD increases as the target RPC specimen location approaches the growth plate and decreases on moving away from the growth plate. The study also indicates that consistency is necessary when obtaining RPC specimens to avoid error due to variation from the specified landmark. Additionally, the BMD decreased as the diameter of the platen is reduced. Choosing platen size then becomes a trade off between testing the greatest amount of cancellous bone possible and potentially higher load sharing by the cortical shell with larger platen sizes as well as the risk of compressing cortical bone during the test.

## ACKNOWLEDGMENTS

I would like to thank Dr. Hogan for all his help and direction. He really made this an enjoyable project and helped me to gain a valuable understanding of bone mechanics. I would also like to thank Dr. Creasy and Dr. Bloomfield for answering questions, giving support, and helping to identify the obvious when I had looked at it too long to notice.

I would like to thank Evan Johnson for taking the time to perform the micro-CT scans as well as helping me understand how to use MicroView. I would also like to thank Jan Stallone for helping obtain bone pictures.

I would also like to thank Ramya, Matt, Kyung Hwa, and Marla for making things enjoyable as well as providing different points of view.

Finally, I would like to thank my wife Celi and daughter Andra for putting up with me and supporting me. They really helped when I needed a break from schoolwork and research.

## TABLE OF CONTENTS

	Page
ABSTRACT .....	iii
ACKNOWLEDGMENTS .....	iv
TABLE OF CONTENTS .....	v
LIST OF FIGURES .....	vii
LIST OF TABLES .....	ix
<b>1. INTRODUCTION .....</b>	<b>1</b>
1.1. Motivation and Rationale .....	1
1.2. Objectives .....	2
1.2.1. Detail Bone Anatomy .....	2
1.2.2. Evaluate RPC Specimen Preparation Procedures .....	3
1.2.3. Evaluate Variation due to Position Differences .....	3
1.2.4. Evaluate Variation due to Platen Size .....	3
<b>2. BACKGROUND .....</b>	<b>4</b>
2.1. General Bone Structure .....	4
2.2. Anatomy of the Rat Femur and Tibia .....	5
2.3. Traditional Methods for Mechanically Testing Rat Cancellous Bone .....	8
2.4. The RPC Test .....	9
2.4.1. Overview .....	9
2.4.2. History .....	10
<b>3. METHODS .....</b>	<b>12</b>
3.1. Experimental Bones .....	12
3.2. Micro-CT Analysis .....	13
3.2.1. MicroView Description .....	13
3.2.2. Bone Orientation in MicroView .....	14
3.2.3. Defining an ROI .....	14
3.2.4. Calculating BMD .....	18
3.3. Detailing Bone Anatomy and Growth Plate Topography .....	19
3.3.1. Correlating Growth Plate Topography to Radiographs and External Landmarks .....	19
3.3.2. Identifying the “Ideal” Cutting Location .....	19
3.4. Changes in Position along the Bone Axis .....	20
3.5. Changes in Platen Diameter .....	21
3.6. Statistical Analysis .....	22
<b>4. RESULTS .....</b>	<b>23</b>
4.1. Identifying the Furthest Extent of the Growth Plate .....	23
4.2. Radiographs versus External Landmarks .....	28

	Page
4.3. New Preparation Procedure.....	29
4.4. Changes in Axial Position.....	30
4.5. Changes in Platen Diameter.....	39
5. DISCUSSION .....	48
5.1. New Specimen Location Method.....	48
5.2. Position.....	48
5.2.1. BMD versus Position .....	49
5.2.2. Percent Change in BMD from Reference Position .....	49
5.2.3. BMD as a Percent of Position Average .....	50
5.3. Diameter.....	50
5.3.1. Percent Change in BMD from 100% Diameter .....	51
5.3.2. BMD as a Percent of Percent Diameter Average.....	52
6. CONCLUSIONS AND RECOMMENDATIONS .....	53
6.1. New RPC Specimen Preparation Procedure .....	53
6.2. Analysis of Variations in RPC Specimen Position and Platen Size.....	53
6.3. Limitations of Results .....	54
6.4. Recommendations for Future Work.....	54
6.4.1. Finite Element Analysis.....	55
6.4.2. Rapid Prototyping.....	55
6.4.3. Improved Cutting Methods.....	55
6.4.4. Improved RPC Positioning .....	56
REFERENCES.....	57
VITA .....	59

## LIST OF FIGURES

	Page
Figure 2.1. Diagram showing the difference between cortical and cancellous bone (after Siegel, 1998). .....	5
Figure 2.2. Contact radiograph of a proximal tibia showing the epiphysis, metaphysis, diaphysis and growth plate. ....	6
Figure 2.3. Micro-CT image of a proximal tibia showing internal anatomy of interest in locating RPC specimens. Features: a, growth plate; b, primary spongiosa; c, transition from primary to secondary spongiosa; d, secondary spongiosa. ....	7
Figure 2.4. RPC test setup. ....	9
Figure 3.1. Sample view of a proximal tibia in MicroView. Yellow region shows ROI placement, size and orientation. (ROI height is 1.992 mm) .....	15
Figure 3.2. Schematic of a tibia and a femur showing approximate location of RPC specimen. ....	16
Figure 3.3. Bottom plane (i.e. most distal) for an ROI of a proximal tibia. Yellow region shows ROI size and placement. ....	17
Figure 3.4. Bottom plane (i.e. most proximal) for an ROI of a distal femur. Yellow region shows ROI size and placement. ....	17
Figure 3.5. Depiction of the differing size of the ROI depending on its axial position in the bone. ....	21
Figure 4.1. Isosurface rendering of a proximal tibia from a micro-CT scan: a, tibial tuberosity; b, top of desired RPC specimen. ....	24
Figure 4.2. Micro-CT image of the sagittal view of a proximal tibia: a, tibial tuberosity; b, top of desired RPC specimen. ....	25
Figure 4.3. Isosurface rendering of a distal femur from a micro-CT scan. The black arrow identifies the most proximal tip of the patellar surface and the most proximal reach of the growth plate. ....	26
Figure 4.4. Micro-CT image of the sagittal view of a distal femur. The white arrow shows the most proximal tip of the patellar surface and the most proximal reach of the growth plate. ....	27
Figure 4.5. Planar contact radiograph of the coronal view of a proximal tibia as previously used for identifying the RPC specimen location. In this specimen, both the bulk (a), as well as the furthest reach, of the growth plate (b) are visible. ....	28

Figure 4.6. Picture of a proximal tibia and a distal femur. The arrows identify the external landmarks and the dashed lines show where the first cut should be made. ....	29
Figure 4.7. Plot of the BMD versus changes in axial position for the bones (tibias) from the HU-PTH study. Each trend line shows the mean BMD and the error bars show the 95% confidence interval on the mean BMD for each group.....	33
Figure 4.8. Plot of the BMD versus changes in axial position for the bones (femurs) from the OVX-IND study. Each trend line shows the mean BMD and the error bars show the 95% confidence interval on the mean BMD for each group.....	34
Figure 4.9. Plot of the percent change in BMD from the reference position versus axial position for the bones (tibias) from the HU-PTH study. ....	35
Figure 4.10. Plot of the percent change in BMD from the reference position versus axial position for the bones (femurs) from the OVX-IND study.....	36
Figure 4.11. Plot of the percent change in BMD from the position average versus axial position for the bones (tibias) from the HU-PTH study. ....	37
Figure 4.12. Plot of the percent change in BMD from the position average versus axial position for the bones (femurs) from the OVX-IND study.....	38
Figure 4.13. Plot of the BMD versus changes in ROI diameter for the bones (tibias) from the HU-PTH study. Each trend line shows the mean BMD and the error bars show the 95% confidence interval on the mean BMD for each group.....	42
Figure 4.14. Plot of the BMD versus changes in ROI diameter for the bones (femurs) from the OVX-IND study. Each trend line shows the mean BMD and the error bars show the 95% confidence interval on the mean BMD for each group. ....	43
Figure 4.15. Plot of the percent change in BMD from the 100% ROI diameter for the bones (tibias) from the HU-PTH study.....	44
Figure 4.16. Plot of the percent change in BMD from the 100% ROI diameter for the bones (femurs) from the OVX-IND study.....	45
Figure 4.17. Plot of the percent change in BMD from the percent diameter average for the bones (tibias) from the HU-PTH study. ....	46
Figure 4.18. Plot of the percent change in BMD from the percent diameter average for the bones (femurs) from the OVX-IND study. ....	47



**LIST OF TABLES**

	Page
Table 3.1. Input parameters for BMD analysis and isosurface rendering.....	18
Table 4.1. P values for a one way ANOVA for variation in BMD with respect to axial position.....	30
Table 4.2. Bone mineral density (in mg/cc) for the bones from both the HU-PTH and OVX-IND studies versus the axial position (in mm) of the RPC specimen location. The bones are sorted by group. Note: an axial position of 0 mm refers to the reference position. ....	32
Table 4.3. P values for a one way ANOVA for variation in BMD with respect to change in ROI diameter. ....	39
Table 4.4. Bone mineral density (in mg/cc) versus the percent reduction in ROI diameter at the reference position. The bones are sorted by group. Data for reductions below 40% are not reported. These values are unreliable due to the small size of the corresponding ROI.....	41

# 1. INTRODUCTION

## *1.1. Motivation and Rationale*

Bone deterioration due to disease (e.g. osteoporosis) and environmental effects (e.g. long-term exposure to microgravity) has created a demand for new or improved treatments to help reverse or prevent bone loss. These treatments usually involve either drugs or rehabilitative exercises to stimulate increased bone formation. The use of animals, such as rats and mice, has become commonplace to help assess the effectiveness of different treatments.

Bone mineral densitometry has become a popular method for assessing bone status in humans due to its non-invasive nature. Bone mineral density (BMD) is a good indicator of the quantity of bone material, but its usefulness and accuracy for assessing bone quality is much debated. Biomechanical testing is thus recommended to evaluate the bone strength and effectiveness of treatments as an essential part of bone studies of animal or cadaveric specimens (Oxlund et al., 2002). However, while the procedures for testing rodent cortical bone are fairly standardized among researchers, the procedures for testing rodent cancellous bone are not. Many of these non-standardized procedures test both cortical and cancellous bone together. This leads to an overestimation of the properties of cancellous bone due to the contributions of the cortical bone (Oxlund et al., 2002; Chachra et al., 2000).

One method that has been introduced for testing only cancellous bone is the reduced platen compression (RPC) test. The RPC test uses two platens with plano-parallel surfaces to compress only the cancellous portion of a 2 mm thick slice taken from either the distal femur or proximal tibia metaphysis of a rat (Rogers, 2002). Recent experiments using the RPC test have raised questions regarding the 2 mm specimen preparation procedures. There has been considerable variability in the specimen location

---

This thesis follows the style of the Journal of Biomechanics.

that can be mostly attributed to a limited understanding of the anatomy of rat long bones and to difficulty in preparation of samples for testing. Additionally, due to slight changes in procedures, as well as inter-technician differences in bone cutting, the target RPC location has varied between studies and between groups within individual studies.

## *1.2. Objectives*

The main goal of this research work is to further develop and improve the procedures for identifying the location of RPC test specimens. These improvements will be aimed at decreasing the amount of time required to complete an RPC analysis and improving the quality of the results obtained from the test. The specific objectives can be completed by the following four tasks:

- Gain a better understanding of the anatomy of the rat proximal tibia and the distal femur
  - Identify the location, shape and orientation (topography) of the growth plate
  - Identify the transition from primary to secondary spongiosa in the metaphysis
  - Correlate these features to either planar radiographs or external landmarks
- Evaluate current RPC test specimen preparation procedures and make recommendations for change
- Evaluate the effect of variations in the actual RPC specimen location from the ideal location on test results
- Evaluate the effect of different platen sizes on test results

### *1.2.1. Detail Bone Anatomy*

Understanding the anatomy of a rat bone and the topography of its growth plate is essential in selecting the “ideal” RPC specimen location. An ideal RPC specimen is comprised of only secondary spongiosa and maximizes the amount of cancellous bone in the specimen. If the RPC specimen is too close to the growth plate, it may contain some of the growth plate as well as primary spongiosa, which do not show the effects of imbalance in bone remodeling. If the specimen is located too far away from the growth plate, there might be very little cancellous bone to test or there might be large holes in the center. Therefore, the “ideal” RPC specimen location should be as close to the growth plate as possible without including growth plate or primary spongiosa.

### *1.2.2. Evaluate RPC Specimen Preparation Procedures*

Current procedures use planar contact radiograph images of the bones to identify the location of the growth plate (Rogers, 2002). Unfortunately, a clear and systematic way to identify the internal location of the growth plate in the intact bone is not well defined. A better understanding of the growth plate topography will improve current RPC specimen preparation procedures by either clarifying how to identify the growth plate on radiograph images or by identifying external landmarks on the bone to locate the RPC specimen below the growth plate.

### *1.2.3. Evaluate Variation due to Position Differences*

In past tests, both the desired RPC specimen location and the actual specimen location have varied. The desired RPC specimen location has varied mainly due to slight modifications in the specimen preparation procedures and subjective factors in identifying the ideal specimen location from radiograph images. Actual specimen location variations are largely due to human error during the cutting of the bone, including both the bone gripping methods as well as difficulty in determining exactly when the bone is properly aligned with the saw blade. Part of the alignment problem comes from the flexibility of the saw blade. It is not currently known how much error this variability adds to the results of the RPC test.

### *1.2.4. Evaluate Variation due to Platen Size*

A platen size of 70% of the largest circle that will fit within the endocortical perimeter (boundary between the cortical wall of the specimen and the cancellous bone) of the RPC specimen is currently used in RPC tests. Given that more cancellous bone is located predominantly near the endocortical surface rather than in the center of the RPC specimen, there is a significant amount of cancellous bone material that is not tested when using a 70% platen size. A good estimate of the amount of loss due to the reduced platen size will help to evaluate the efficacy of the RPC test.

## 2. BACKGROUND

### *2.1. General Bone Structure*

Bone is a combination of both hard and flexible components. The flexible component is a fibrous protein called collagen. The collagenous matrix is mineralized with hydroxyapatite, a form of calcium phosphate. This unique combination of hard and resilient components makes bone very resistant to both tensile and compressive forces and gives it the hardness, rigidity and flexibility needed to provide support for the usual loading conditions that bone is exposed to (Siegel, 1998; White, 2000).

Bone can be separated into two categories, cortical and cancellous, which are mainly distinguished by the porosity of the bone, as the molecular and cellular compositions of each type are identical. Figure 2.1 shows a depiction of the difference between cortical and cancellous bone. Compact, or cortical, bone is very dense and provides the majority of support for the skeletal structure. It is found in large quantities in the walls of bone shafts and on external bone surfaces such as the midshaft of long bones where torsional and bending stresses are the greatest. Spongy, or cancellous, bone is very porous with a lightweight honeycomb structure. It is composed of struts and plates called trabeculae (Latin, means little beams) that help provide support for stresses resulting from walking, running, and jumping. Cancellous bone is always connected to cortical bone and is found under protuberances where tendons attach, in vertebral bodies, in the ends of long bones, and inside short and flat bones. It provides support by efficiently transmitting loads to the cortical bone while using a minimum amount of bone material. Because of its large surface area to volume ratio, cancellous bone responds more rapidly to nutritional, hormonal or environmental changes than does cortical bone making it more susceptible to fracture or other problems. Additionally, cancellous bone is more compliant than cortical bone and serves to absorb energy and hence is often found near joints (White, 2000; Siegel, 1998; Ogden, 1980).

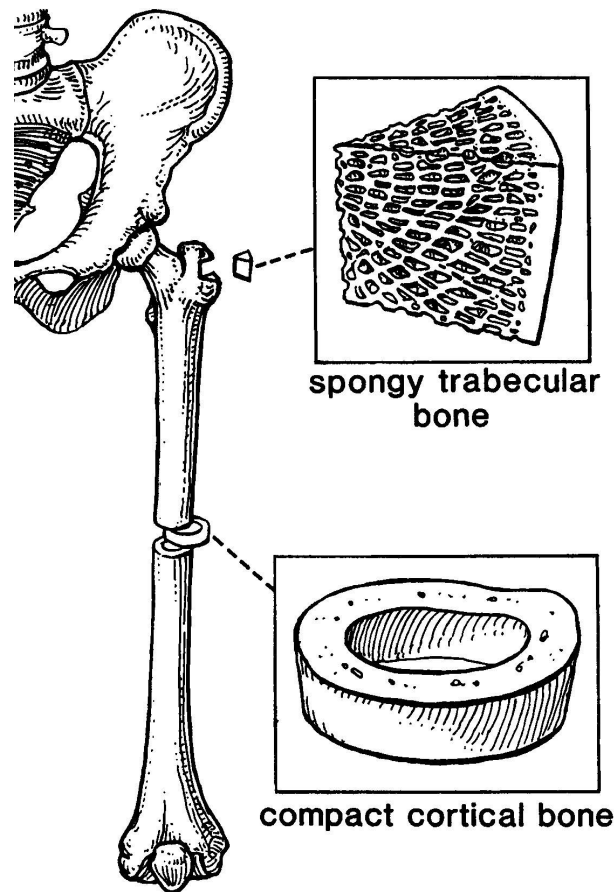


Figure 2.1. Diagram showing the difference between cortical and cancellous bone (after Siegel, 1998).

## 2.2. Anatomy of the Rat Femur and Tibia

Rat long bones (tibia and femur) as a whole have four major features, which are identified on a contact radiograph image of a proximal tibia in figure 2.2. The ends are called epiphyses and their surfaces are parts of joints. The long shaft or mid-section of the bone is called the diaphysis and is made solely of cortical bone. Between the diaphysis and the epiphysis lies an expanded, flared region called the metaphysis that is made of cancellous bone surrounded by a thin cortical shell. Finally, a thin layer of highly organized cartilage called the growth plate separates the metaphysis and epiphysis (White, 2000; McLean and Urist, 1968).

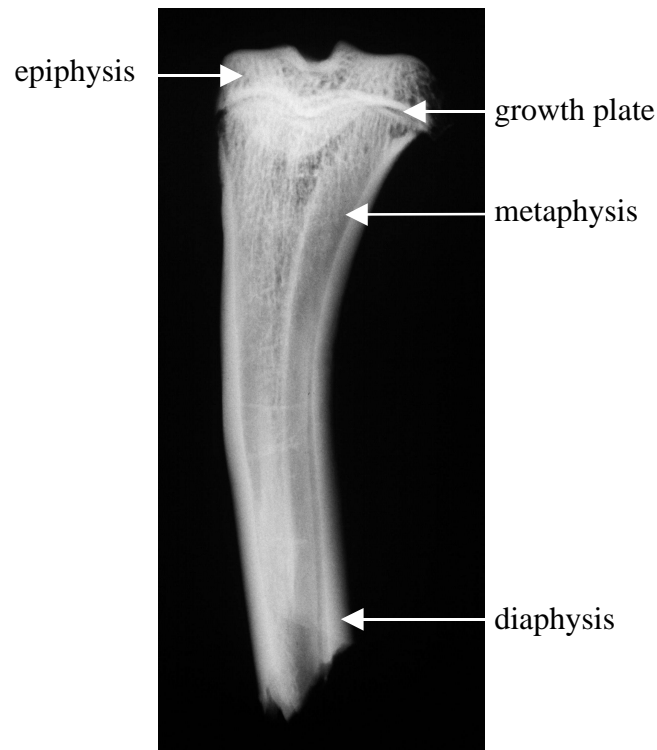


Figure 2.2. Contact radiograph of a proximal tibia showing the epiphysis, metaphysis, diaphysis and growth plate.

During growth, long bones increase in length through the growth plate, a cartilaginous layer that adds new bone on the metaphyseal border in long spicules called trabeculae, which are largely cartilage in composition. Over time these cartilaginous spicules become fully mineralized and then undergo normal remodeling activity. This newly mineralized bone formed near the growth plate cartilage is called primary spongiosa. This process continues until the time that the bone reaches its final adult length and the metaphysis and epiphysis fuse together (White, 2000; Ogden, 1980).

After the cartilage surrounding the primary spongiosa is fully mineralized, the primary spongiosa is subject to normal bone remodeling. Eventually, the form of the primary spongiosa is completely remodeled into a new structure known as the secondary spongiosa. The layout of the growth plate, primary and secondary spongiosa is identified in the micro-CT image in figure 2.3 (Kimmel, 1991; McLean and Urist, 1968; Vico et al., 1991).

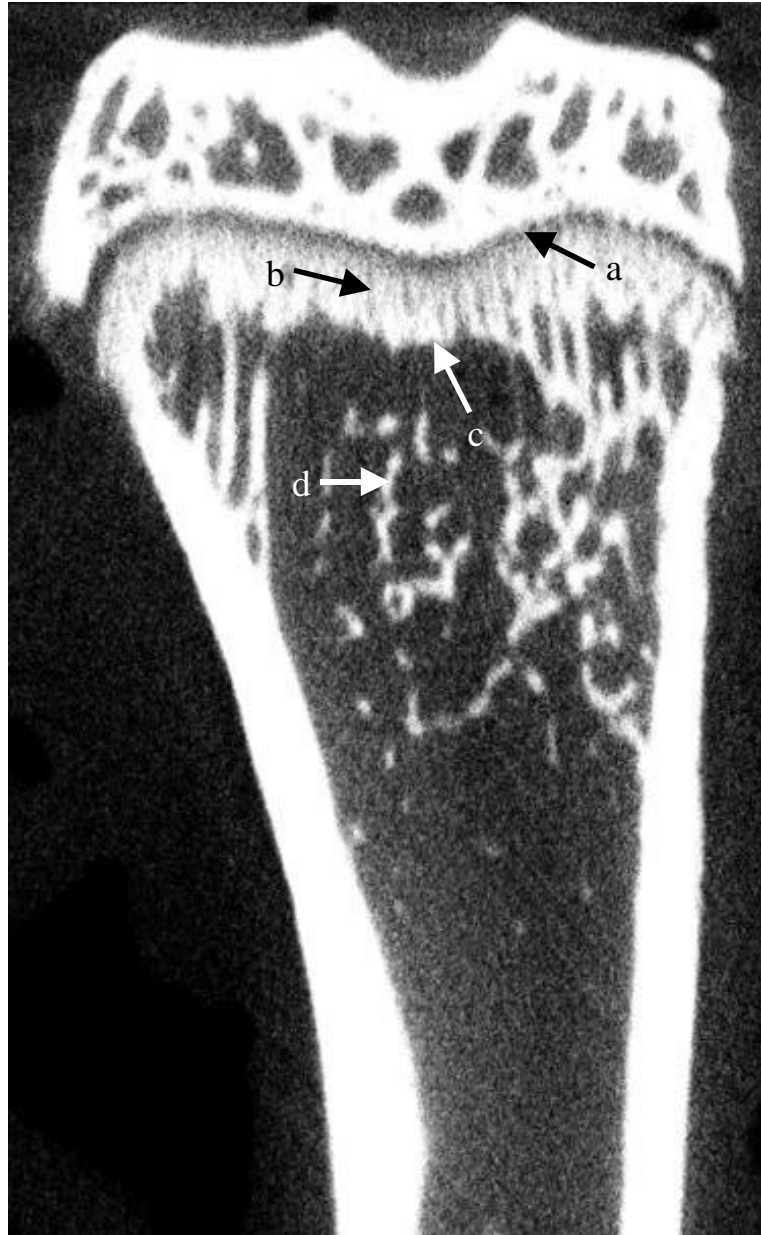


Figure 2.3. Micro-CT image of a proximal tibia showing internal anatomy of interest in locating RPC specimens. Features: a, growth plate; b, primary spongiosa; c, transition from primary to secondary spongiosa; d, secondary spongiosa.



### *2.3. Traditional Methods for Mechanically Testing Rat Cancellous Bone*

Cancellous bone is often emphasized more heavily than cortical bone in bone studies for several reasons. Cancellous bone is more responsive to bone remodeling imbalances as well as to treatment. Therefore, cancellous bone usually shows a greater response than cortical bone. In people and animals with bone deterioration, fractures almost always occur at sites where there are large amounts of cancellous bone, such as vertebrae and the femoral neck.

One of the more common methods for testing cancellous bone involves compressing entire vertebrae. This method uses two parallel plates to compress the vertebrae (Ke et al., 1998; Mosekilde et al., 1998). While vertebrae do contain cancellous bone, this method also tests the cortical bone surrounding the cancellous bone. Some researchers (Chachra et al., 2000) have gone as far as coring the cancellous bone out of the vertebrae and comparing it to whole vertebrae to better estimate the properties of cancellous bone. Coring the cancellous bone results in a 20% drop in ultimate compressive strength. Others (Bauss et al., 2002) remove the arch and transverse processes as well as the cortical endplates prior to testing.

The femoral neck is another bone site commonly used for testing cancellous bone. The femoral neck is one of the more common sites for osteoporotic bone fractures in humans and contains large portions of cancellous bone. Testing of the femoral neck is usually done using compression or cantilever bending (Ke et al., 1998; Mosekilde et al., 1998; Stenstrom et al., 2000). Femoral neck fractures typically occur through either the middle part of the femoral neck or towards the base. The loading in this area is a combination of bending, compression and shear.

Another method for testing cancellous bone involves indenting the metaphysis (from distal femur for example) of a long bone with a cylindrical indenter or platen. The specimen is cut from the metaphysis at a set distance (e.g. 4 mm) from the end of the bone (either distal femur or proximal tibia). The platen is usually the same size (e.g. 1.6 mm diameter) for all bones tested and is usually inserted a pre-set (e.g. 2 mm) distance (Ke et al., 1998).

## 2.4. The RPC Test

The reduced platen compression (RPC) test is a method that was developed to approximate testing of only cancellous bone from rats. The RPC test has the advantage over traditional methods for testing cancellous bone in that only cancellous bone is tested directly, although cortical bone remains a part of the specimen and influences results.

### 2.4.1. Overview

The RPC test involves several steps that determine the mechanical properties of cancellous bone from either the rat distal femur or proximal tibia. A schematic of the test setup is shown in figure 2.4.

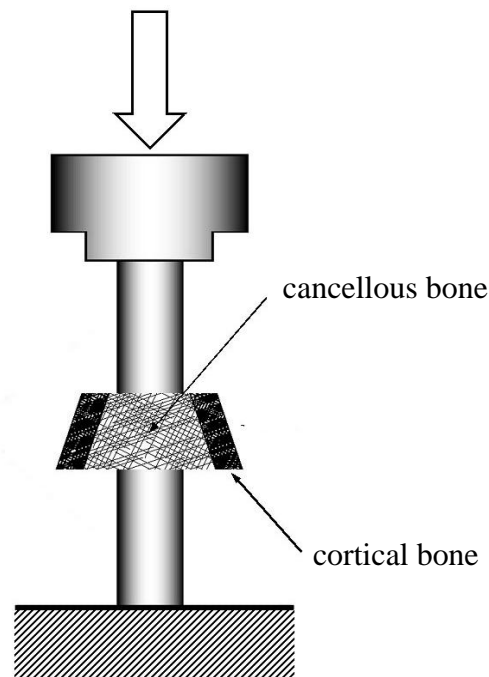


Figure 2.4. RPC test setup.

First, contact radiographs of the coronal view of each bone are taken using a General Electric Industrial Radiograph Machine (General Electric, Lexington, MA) on Kodak X-

Omat TL Film (Eastman Kodak Company, Rochester, NY). These radiographs are then mounted on slides and digitized using a Polaroid SprintScan 35 slide scanner (Polaroid Corporation, Cambridge, MA). The images are analyzed to determine the furthest extent of the epiphyseal growth plate thereby identifying the desired RPC specimen location. The distance from the end of the bone to the RPC specimen location (first cut distance) is found using SigmaScan Image (Version 1.2, Jandel Scientific Software, San Rafael, CA). The 2 mm thick RPC specimen is then cut from the bone using an Isomet low-speed diamond blade saw (Buehler LTD, Lake Bluff, IL). Contact radiographs of the RPC specimen are then made and analyzed to determine the largest circle that will fit inside the endocortical perimeter of the RPC specimen. The platen size is determined by taking 70% of the diameter of this circle. Then, the RPC specimen is compressed with the corresponding platens in an Instron model 1125 mechanical testing machine with Labtech Notebook Pro Software Version 8.01 (Laboratory Technologies Corporation, Wilmington, MA) recording the data. The data are analyzed following traditional compression test analysis techniques (Rogers, 2002).

#### *2.4.2. History*

The reduced platen compression (RPC) test was first introduced as a method for testing the mechanical properties of cancellous bone from the proximal tibia of the rat (Rhumann, 1998). Specimens were obtained by cutting a 2-mm thick slice perpendicular to the bone axis and just distal to the proximal growth plate from both the left and right tibia of each rat. The specimen from one leg was compressed using the RPC test method and the specimen from the other leg was tested using the whole slice test method (where the entire test specimen was compressed, including the cortical shell). A standard platen diameter of 3 mm was used for all of the RPC tests. The differences in the results produced by the two methods showed that the whole slice method yielded higher values for mechanical properties (e.g. up to a 63% increase in maximum stress) than did the RPC method (Ruhmann, 1998).

Specimens were located by analyzing contact radiograph images of the tibia to estimate the location of the growth plate and the distal extent of the cancellous bone. The ratios between the length from the distal end of the tibia to the distal end of the estimated 2-mm test specimen and the total length of the tibia from each bone were averaged. This average was then used to locate the actual test specimen used in the experiment (Ruhmann, 1998).

Further improvements of the RPC test determined specimen locations through analysis of radiograph images of each individual bone instead of using a percentage of the bone length. Using distal femur samples, the RPC specimen locations were found for each bone by digitizing and analyzing radiograph images of the coronal view of the distal femur to determine the proximal extent of the distal growth plate. The test procedures were also changed to allow for different size platens to accommodate the individual bone sizes. Tracing the endocortical perimeter from a digitized radiograph image of each RPC specimen determined the platen size for each specimen. The platen size was defined as 75% of the minor axis of the area enclosed by the endocortical perimeter (Nguyen, 2001).

The RPC specimen location procedure was further improved by comparing two proximal tibias (both cut longitudinally in half through either the coronal or sagittal plane) with radiograph images of both the coronal and sagittal views of each bone. This helped to identify the growth plate region of each bone on the corresponding radiograph image. Platen size was defined by determining the largest circle that would fit inside the RPC specimen's endocortical perimeter on a radiograph image and setting the platen size as 70% of that diameter. An evaluation of the effect of different sized platens was performed by using a simplified finite element model (Rogers, 2002).

Despite all the improvements that have been made, there still remains significant subjectivity in selecting an RPC specimen location. This is mainly due to an incomplete understanding of rat bone anatomy, especially regarding the growth plate. This subjectivity has caused variation in where the RPC specimens have been taken in past studies.

### 3. METHODS

#### 3.1. *Experimental Bones*

Bones from two different studies are used in this thesis. One set of bones comes from a study looking at the effect of parathyroid hormone on bone and muscle recovery for male Sprague-Dawley rats subject to 28 days of hindlimb unloading and 28 days of normal cage activity (HU-PTH) performed at Texas A&M University (College Station, TX). Twelve tibias are available for analysis from this study. The second set of bones comes from a study looking at the effect of an 8 week indomethacin treatment on ovariectomized female Sprague-Dawley rats (OVX-IND) performed at the University of Texas M.D. Anderson Cancer Center (Houston, TX). Thirty one femurs are available for analysis from this study.

Given the objectives of this study, it is desirable to investigate bones having a wide range of properties (BMD). It is also desirable to investigate properties from both femurs and tibias. This makes the findings as generally applicable as possible. As such, bones covering a wide range of BMD as well as bones from differing groups within a study are analyzed.

The HU-PTH study has three groups (4 bones per group), baseline control (sacrificed at end of unloading), vehicle treatment (VEH) and parathyroid hormone treatment (PTH). Both the VEH and PTH group are sacrificed after 28 days of treatment administered at the end of the unloading period. There is no statistically significant difference between the proximal tibia metaphysis BMD of the baseline control group and the VEH group, so only the bones from the VEH group and the PTH group are analyzed in this work. This helps to demonstrate differences that exist between two different groups within a study. The bones in the OVX-IND study have a fairly random spread in the BMD data (from micro-CT scans) from the 31 bones with no clear separation between groups. Nine bones are used from this study, the three highest BMD

(HIGH), the three lowest BMD (LOW), and the three median BMD (MED). This is done to show how bones with high, medium and low BMD compare to each other.

### *3.2. Micro-CT Analysis*

Micro-CT scans of rat long bones (31 femurs and 12 tibias) are obtained using a high-resolution micro-CT scanner (eXplore RS-9 micro-CT scanner, GE Medical Systems) located at the University of Texas M.D. Anderson Cancer Center. The bones are wrapped in gauze wetted with saline solution during scanning. The scanner is set at the highest resolution (27 microns) with the x-ray tube voltage set at 50kVp with the current maintained at 1mA. The scanned images are reconstructed with proper calibration to Hounsfield Units. The micro-CT technician at the M.D. Anderson Cancer Center performs the scans; the author has no involvement or control in the scanning process.

One advantage of using micro-CT images to map bone anatomy is that it produces high-resolution three-dimensional databases that can be viewed and manipulated to look at specific regions of the bone. Another advantage is that micro-CT imaging does not damage the bone, which can then be analyzed using the RPC test. One main disadvantage of micro-CT scans is that they only show mineralized bone; other unmineralized features such as cartilage are not visible.

#### *3.2.1. MicroView Description*

MicroView (version 1.1.1, GE Medical Systems) is the program used to view and analyze micro-CT scans from the eXplore-RS micro-CT scanner. A micro-CT scan is opened in MicroView as a three-dimensional field of voxels (a three-dimensional pixel). Each voxel has a grayscale intensity value set during the scanning process. The bone is seen by the contrast between high intensity voxels and low intensity voxels. In MicroView, three planes are defined and only the voxels that lie within those planes are shown. Figure 3.1 shows a sample view of a micro-CT scan of a proximal tibia. The positions of each plane can be moved so that each slice of the scan can be viewed.

### *3.2.2. Bone Orientation in MicroView*

When the micro-CT scans are reconstructed prior to viewing in MicroView, the bone is oriented based on its placement relative to the scanner during the scan. This orientation is frequently different than what is needed for the RPC analysis. To correct this, the bones are reoriented in MicroView using the “Reorient Image” tool. Once the scan is open in MicroView, the visible planes can be reoriented in two different manners. First, placing the mouse cursor on the edge of the plane, pressing and holding the middle mouse button, and moving the mouse will rotate the planes about the axis parallel to the selected edge and passing through the selected plane. Second, placing the mouse over the corner of a plane, pressing and holding the middle mouse button, and moving the mouse will rotate the planes about the axis perpendicular to the selected plane. Once the planes have been oriented so that generated ROI will be aligned with the long axis of the bone, the orientation can be exported to a new file.

### *3.2.3. Defining an ROI*

MicroView allows for the definition of a 3-dimensional rectangular or elliptical region of interest (ROI), which can be analyzed to calculate various bone parameters such as BMD. Manipulating the size and position of the ROI facilitates easy evaluation of changes in cancellous bone properties within each micro-CT scan. It also facilitates specimen-to-specimen comparisons. The ROI is defined by size dimensions and three-dimensional position coordinates. A sample ROI can be seen as the yellow cylindrical shaped region in figure 3.1.

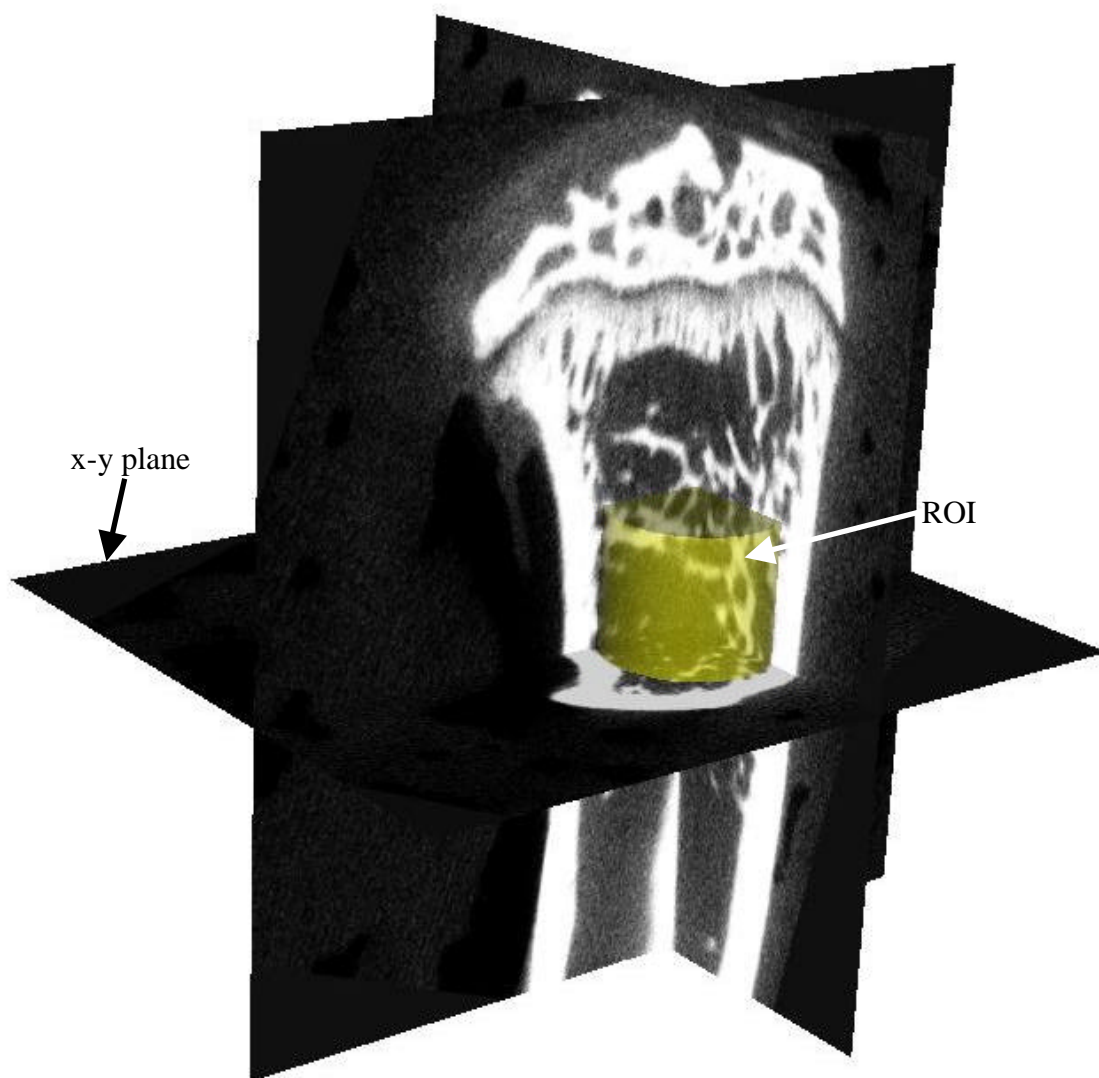


Figure 3.1. Sample view of a proximal tibia in MicroView. Yellow region shows ROI placement, size and orientation. (ROI height is 1.992 mm)

For each individual RPC specimen location, the ROI is set by first positioning the x-y plane (perpendicular to the long axis of the bone) so that it is aligned with the top of the “ideal” specimen location. The top surface of the ROI is then aligned with this plane. Next the ROI height is set to 2 mm (The actual height is 1.992 mm due to voxel size). The x-y plane is then moved so that it is aligned with the bottom of the ROI. The



diameter and x, y coordinates of the ROI are then set so that the ROI boundaries are tangent to the endocortical perimeter. In other words, the ROI is positioned so that the largest possible diameter is achieved without including any cortical bone in the ROI. Figure 3.2 shows a depiction of where the top and bottom planes of an ROI are located on both a tibia and a femur.

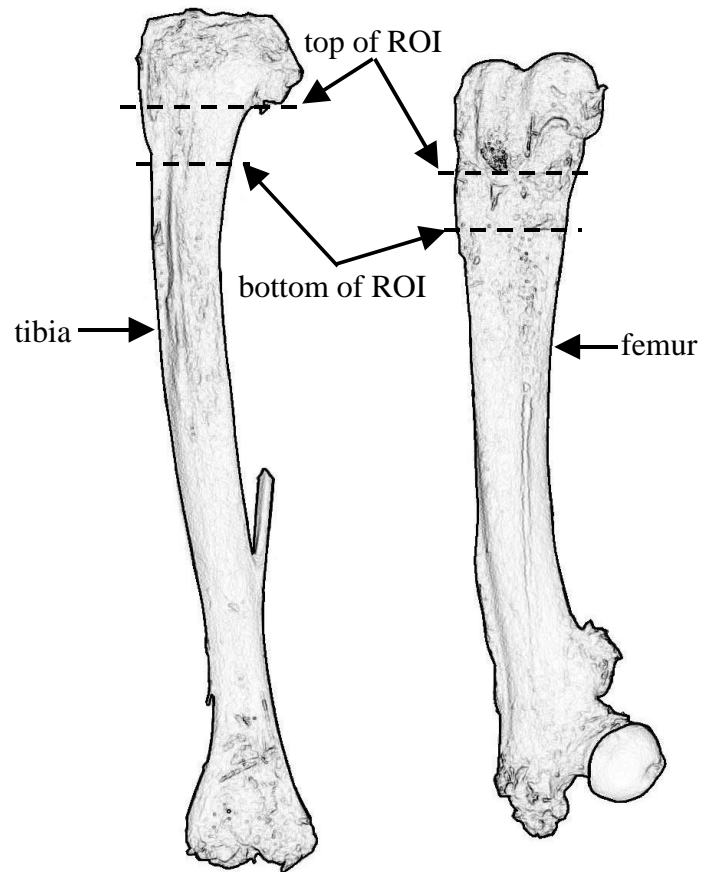


Figure 3.2. Schematic of a tibia and a femur showing approximate location of RPC specimen.

Figures 3.3 and 3.4 show the bottom plane from a micro-CT scan of the desired RPC specimen location for a tibia and a femur, respectively. The yellow circle in the middle shows how the ROI has been sized and placed to achieve the largest size possible without including any cortical bone.

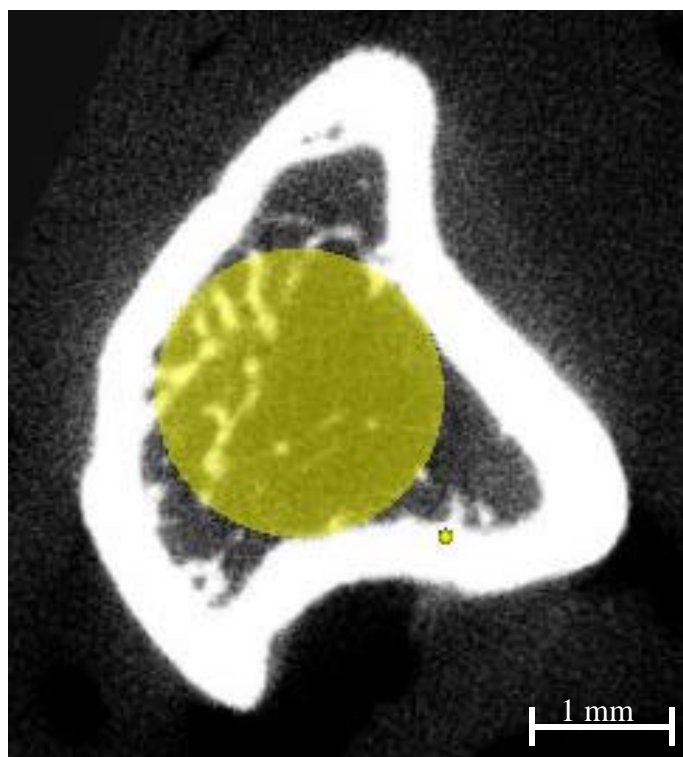


Figure 3.3. Bottom plane (i.e. most distal) for an ROI of a proximal tibia. Yellow region shows ROI size and placement.

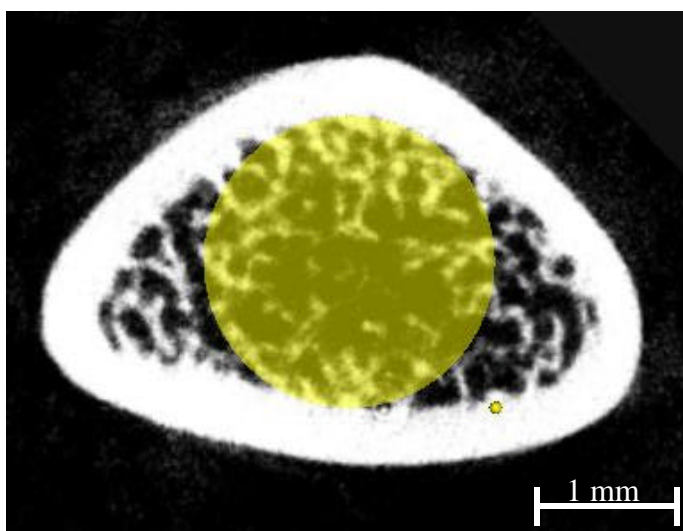


Figure 3.4. Bottom plane (i.e. most proximal) for an ROI of a distal femur. Yellow region shows ROI size and placement.

### 3.2.4. Calculating BMD

MicroView has various tools for analyzing the bone within a defined ROI. One tool, BMD Analysis Tool, calculates the bone mineral density (BMD). This tool requires three user inputs for calculating the BMD, “bone ADU,” “water ADU,” and “exclusion ADU”. These parameters help the program identify the difference between bone, water, and air based on the intensity of each voxel within the scan. Another useful feature of MicroView is the isosurface-rendering tool. This tool uses the micro-CT image file to generate a three-dimensional surface rendering of the scanned object. The isosurface rendering is very useful in relating internal bone structures and features to external landmarks. It is also beneficial for simply understanding what the three planar slices normally show in MicroView. The isosurface rendering tool requires a “Threshold” input to generate the surfaces. The values used for the required inputs for both the femurs and the tibias are shown in table 3.1. These values are based on recommendations from the micro-CT scanner technician and by plotting the voxel intensity of a line passing through the bone to help identify the minimum voxel intensity that still represents bone.

Table 3.1. Input parameters for BMD analysis and isosurface rendering.

Input Parameter	Bone Type	
	Femur	Tibia
Bone ADU	1000	3000
Water ADU	0	0
Exclusion ADU	500	1000
Threshold	500	1000

The difference between the values used for the femurs and the tibias is due to a change in the scanner calibration after scanning the femurs and before scanning the tibias. Unfortunately, the values for BMD cannot be compared between the tibias and femurs because of the difference in input settings. However, the trends seen from the analysis can still be compared.

### *3.3. Detailing Bone Anatomy and Growth Plate Topography*

The micro-CT images are used to explore the 3-dimensional bone anatomy and topography of the growth plate of both femurs and tibias. Significant features of the bone, such as the growth plate and the transition from primary to secondary spongiosa, are identified. This develops a good understanding of the location, shape, extent and orientation of both the growth plate and the primary spongiosa, which aids in selecting an ideal RPC specimen location.

#### *3.3.1. Correlating Growth Plate Topography to Radiographs and External Landmarks*

Using micro-CT images to locate the desired RPC specimen location for every bone that needs to be tested is a very time consuming process. A single bone scan takes several hours and the scanner is only available on a limited basis. For this reason, the knowledge gained from mapping the topography of the rat bone growth plate will be correlated with a more practical method for identifying the RPC specimen location.

Two methods for locating the RPC specimen are explored. First, the continued use of contact radiographs to identify the extent of the growth plate and secondary spongiosa is evaluated. Second, an attempt is made to correlate knowledge gained from the micro-CT scans to easily identifiable external landmarks on the bones.

#### *3.3.2. Identifying the “Ideal” Cutting Location*

Upon relating bone topology to contact radiographs or to external landmarks, the current RPC specimen preparation procedures are evaluated. Recommendations are sought for an “ideal” location for RPC specimens. These recommendations include details on how to identify the ideal RPC specimen location using either radiographs or landmarks so that someone who has not analyzed the micro-CT images can easily and accurately identify the RPC specimen location.

### *3.4. Changes in Position along the Bone Axis*

The variation in mechanical properties with respect to changes in the target RPC specimen location along the long axis of the bone is evaluated using BMD as a surrogate for the mechanical properties obtained through the RPC test (Bauss et al., 2002; Ito et al. 2002).

First, the “ideal” RPC specimen location (from section 3.3.2, call this the “reference” position) is analyzed by defining an ROI with the largest diameter possible for the test region and calculating BMD. The target location for the RPC specimen is then moved from the reference position (both directions along the bone axis) in small increments of 0.204 mm, up to 1.02 mm in both directions. At each location, the ROI position and diameter are redefined to correspond to the new RPC specimen location. At each location, the BMD is found for the ROI corresponding to the region that would be tested if that were the actual RPC specimen. The BMD values for each location are then analyzed to estimate how much the mechanical properties are affected by moving the RPC specimen location.

Again, the cross section of the ROI farthest from the growth plate is set to inscribe the endocortical perimeter and thus determines the diameter of the ROI. Therefore, ROI's that are closer to the growth plate are larger than the reference ROI and the ROI's farther from the growth plate are smaller. This is due to the flaring of the bone and is depicted in figure 3.5.

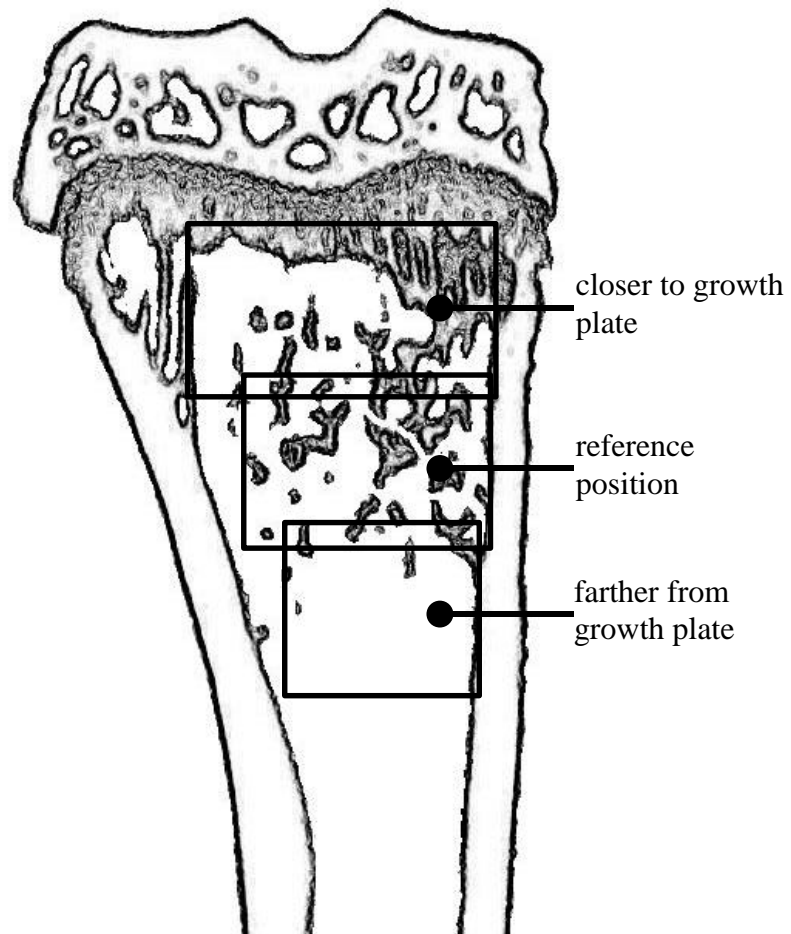


Figure 3.5. Depiction of the differing size of the ROI depending on its axial position in the bone.

### 3.5. Changes in Platen Diameter

For this part of the analysis, the reference RPC specimen location is used. First the ROI is defined so that its diameter is one hundred percent of the diameter of the largest circle that fits inside the endocortical boundary of the specimen. Then the diameter is reduced in ten percent increments of the largest diameter (i.e. 100%, 90%, 80%, etc.) while maintaining the same center for the cylinder. Again, MicroView only allows dimension changes to occur per voxel, so the percent reduction in diameter is not necessarily in exact ten percent increments, but it is as close as possible. At each

location the BMD is found. The BMD values for each ROI diameter are compared to evaluate the effect of changes in the platen size on the RPC test results.

### *3.6. Statistical Analysis*

A one way ANOVA is used to test if BMD varies with respect to changes in the axial position or with respect to reductions in ROI diameter. For each case the change in BMD is analyzed using either the change in position or the change in ROI diameter as the independent variable. The results for each group (i.e. PTH group, VEH group, etc.) are analyzed separately so only one variable changes. The results are considered significant when  $p \leq 0.05$  (Montgomery, 2001).

## 4. RESULTS

### 4.1. Identifying the Furthest Extent of the Growth Plate

Using MicroView to explore the growth plate topography and its relation to the whole bone anatomy shows that on the tibias and the femurs, the growth plate has a fairly irregular undulated shape. The most important feature of the growth plate in both cases is that the growth plate curves down to a point on the anterior aspect of the bone. This point marks either the most distal or most proximal reach of the growth plate on the proximal tibia or distal femur respectively and the point at which the top of an ideal RPC specimen should be located. On both the proximal tibia and the distal femur, this point can be related to easily identifiable external landmarks.

The landmark on the proximal tibia that shows the most distal reach of the growth plate is the base of the tibial tuberosity (where the patellar ligament of the *quadriceps femoris muscle* inserts) on the anterior side of the bone (McLean and Urist, 1968; White, 2000). Figure 4.1 shows an isosurface rendering of a proximal tibia from a micro-CT scan with the tibial tuberosity and the top of the desired RPC specimen identified. Figure 4.2 shows a slice (sagittal view) from the same micro-CT scan taken through this landmark. This view clearly shows how the growth plate curves down making it the most distal reach of the growth plate.

A similar landmark for the femur is the most proximal tip of the patellar surface on the anterior side of the bone (White, 2000). Figure 4.3 shows an isosurface rendering of a distal femur from a micro-CT scan with the tip of the patellar surface identified. Figure 4.4 shows a slice (sagittal view) from the same micro-CT scan taken through this landmark. This view clearly shows how the growth plate curves down to meet the tip of the patellar surface making it the most proximal reach of the growth plate.



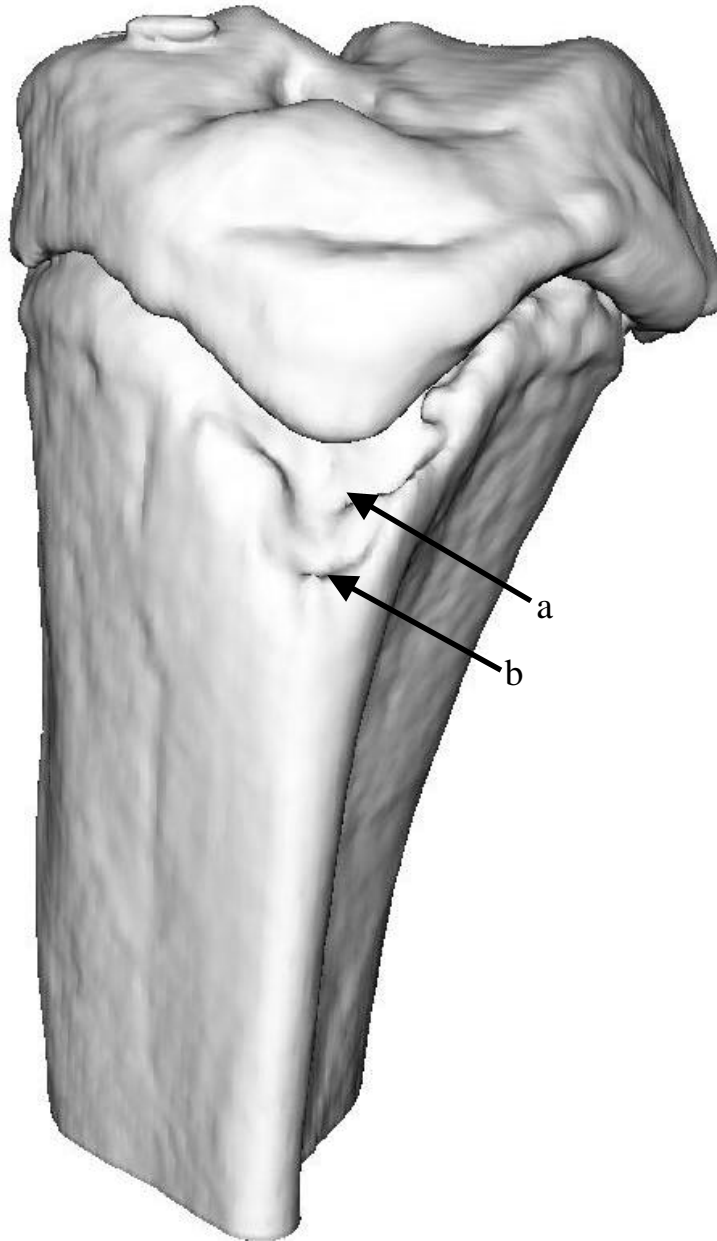


Figure 4.1. Isosurface rendering of a proximal tibia from a micro-CT scan: a, tibial tuberosity; b, top of desired RPC specimen.

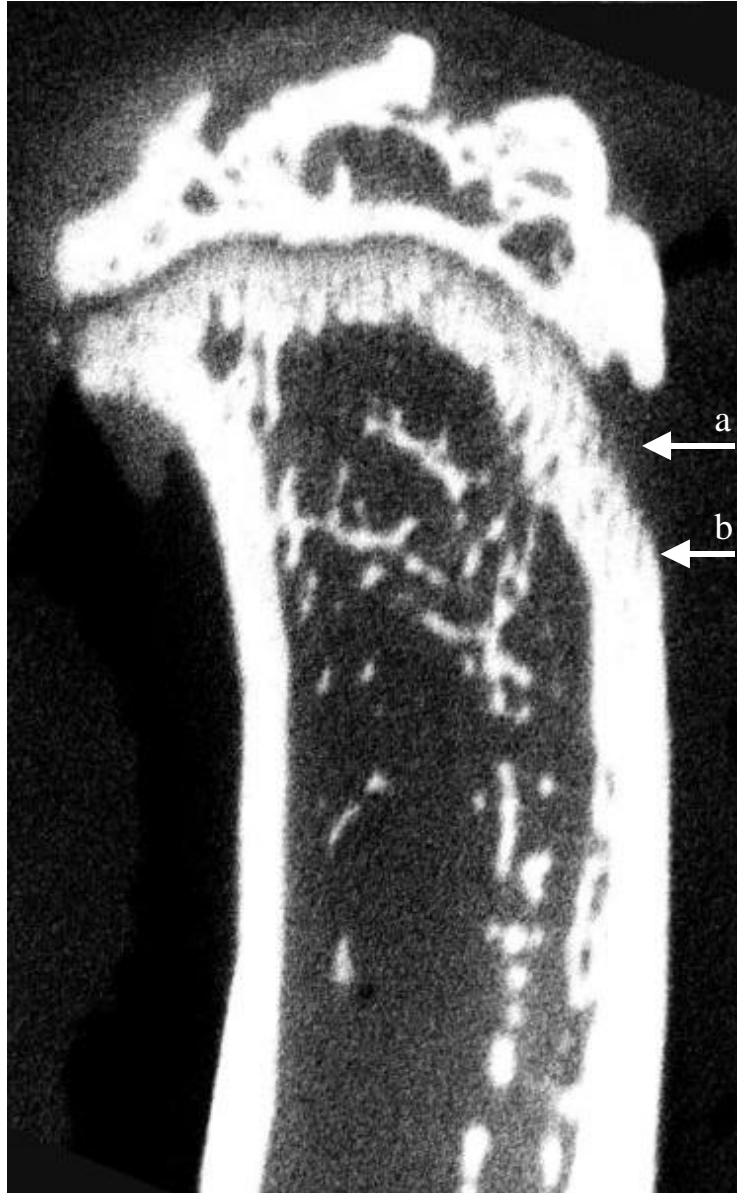


Figure 4.2. Micro-CT image of the sagittal view of a proximal tibia: a, tibial tuberosity; b, top of desired RPC specimen.

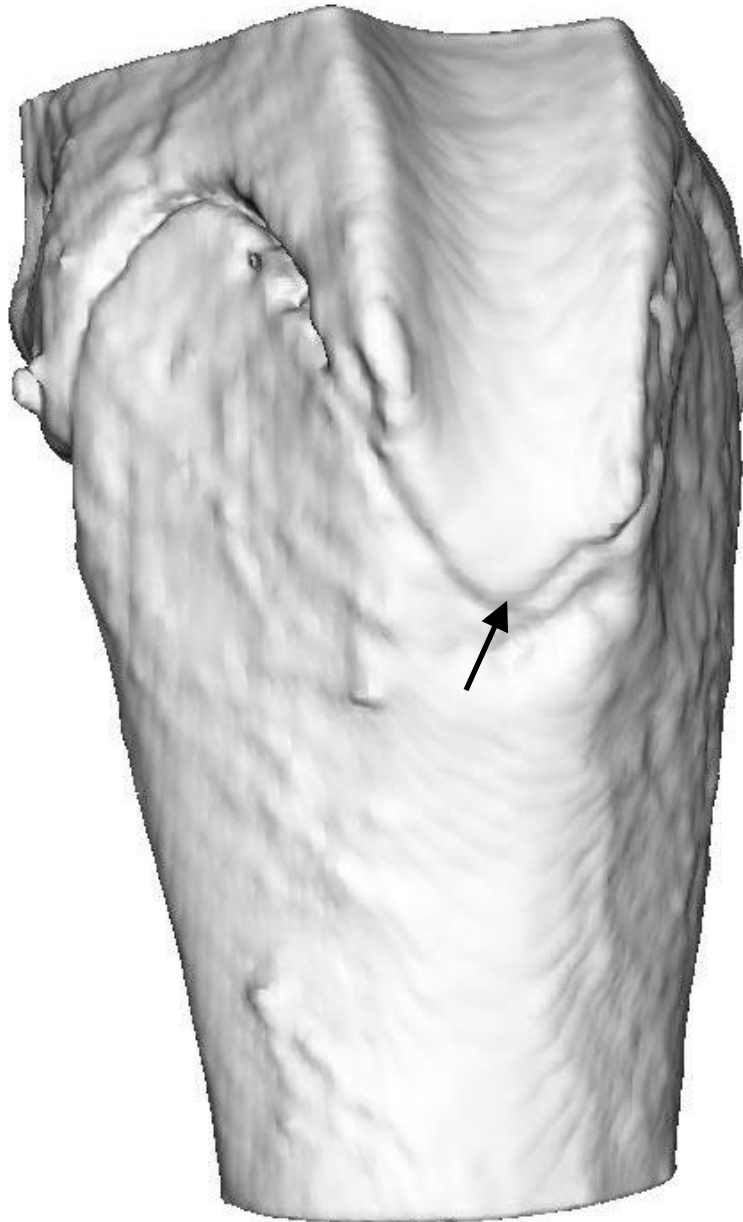


Figure 4.3. Isosurface rendering of a distal femur from a micro-CT scan. The black arrow identifies the most proximal tip of the patellar surface and the most proximal reach of the growth plate.



Figure 4.4. Micro-CT image of the sagittal view of a distal femur. The white arrow shows the most proximal tip of the patellar surface and the most proximal reach of the growth plate.

#### 4.2. Radiographs versus External Landmarks

One difficulty that has arisen with the use of radiographs is clearly and easily identifying the most distal/proximal part of the growth plate. This part as shown by the micro-CT images is typically only seen on radiographs as a light cloud (tibia) as seen in figure 4.5. On some specimens, this cloud is not even distinguishable. The growth plate is even more difficult to identify on radiographs of the femur. Due to the difficulty of identifying the full shape of the growth plate on radiographs and the ease of using external landmarks, correlating the micro-CT scans to radiographs is not pursued as a useful method for improving RPC specimen location procedures.

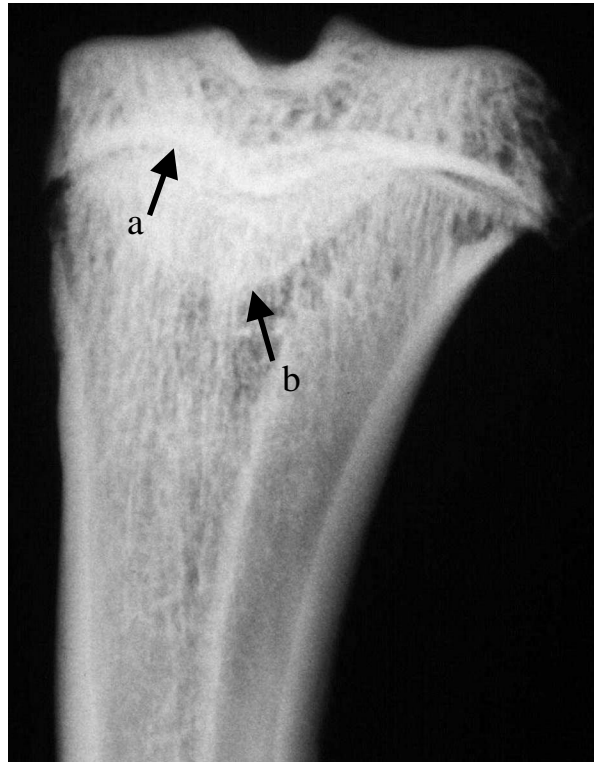


Figure 4.5. Planar contact radiograph of the coronal view of a proximal tibia as previously used for identifying the RPC specimen location. In this specimen, both the bulk (a), as well as the furthest reach, of the growth plate (b) are visible.

### 4.3. New Preparation Procedure

The new recommended procedure for locating and preparing RPC specimens uses external landmarks instead of contact radiographs to identify the specimen. The previously identified landmarks for the tibia and femur identify the top plane of the desired RPC specimen and are identified in the photograph in figure 4.6. The specimens should be cut from the bone so that the saw blade touches the landmark with the width of the blade passing on the growth plate side of the landmark. The RPC specimen is then finished by moving the bone 2.4 mm (the 0.4 mm is to account for the thickness of the blade) and cutting through the bone a second time.



Figure 4.6. Picture of a proximal tibia and a distal femur. The arrows identify the external landmarks and the dashed lines show where the first cut should be made.

#### 4.4. Changes in Axial Position

The analysis of the effect of changing the RPC specimen location on BMD shows that the BMD increases as the target RPC specimen location approaches the growth plate and decreases as the RPC specimen location moves away from the growth plate. Again, the RPC specimen location was moved in small increments from the reference position both towards and away from the growth plate. It is interesting to note that from the one-way ANOVA all groups except the VEH group varied significantly with respect to the RPC specimen location. The p values from the ANOVA are given in table 4.1.

Table 4.1. P values for a one way ANOVA for variation in BMD with respect to axial position.

<u>group</u>	<u>P</u>
PTH	6.328E-07
VEH	1.260E-01
LOW	4.576E-10
MED	8.514E-11
HIGH	3.733E-06

Table 4.2 shows the data for the analysis of varying the axial position of the RPC specimen location for all of the bones. Figures 4.7 and 4.8 plot the BMD versus axial position for the HU-PTH study and OVX-IND study, respectively. Note that an axial position of zero is the reference RPC specimen location. A positive axial position is closer to the growth plate than the reference position and a negative axial position is farther away. The trend lines and error bars show the mean BMD and 95% confidence interval for each group.

Two methods of normalizing the data with respect to BMD are presented. Both of these normalizations are presented to help demonstrate how the BMD varies with axial position within the bone. First, the BMD values are expressed as a percent change in BMD from the reference position. In other words, for each bone the percent change at each axial position is found by the following expression,

$$\% \text{ change} = \frac{BMD_{\text{position}} - BMD_{\text{ref}}}{BMD_{\text{ref}}} \cdot 100 \quad \text{Equation 4.1.}$$

where  $BMD_{\text{position}}$  is the BMD value for the bone at the specified axial position and  $BMD_{\text{ref}}$  is the BMD from the reference position (axial position = 0). The percent change in BMD versus axial position is shown in figures 4.9 and 4.10.

Second, the BMD is expressed as a percent change from the position average. In other words, for each axial position (e.g. axial position = 0.6 mm), the average BMD for all of the bones at that axial location within each study is found ( $BMD_{\text{average}}$ ) and the data is expressed as a percent change from this average. The percent change from the position average is then found by,

$$\% \text{ average} = \frac{BMD_{\text{position}} - BMD_{\text{average}}}{BMD_{\text{average}}} \cdot 100 \quad \text{Equation 4.2.}$$

The data for this normalization are shown in figures 4.11 and 4.12. Note that the numbers for each bone are the rat subject numbers assigned at the beginning of each study. As such, in this thesis they only serve the purpose of identifying each individual bone on the graphs and tables.



Table 4.2. Bone mineral density (in mg/cc) for the bones from both the HU-PTH and OVX-IND studies versus the axial position (in mm) of the RPC specimen location. The bones are sorted by group. Note: an axial position of 0 mm refers to the reference position.

		Tibiae										
		Axial position										
Spec. No.		-1.0	-0.8	-0.6	-0.4	-0.2	0.0	0.2	0.4	0.6	0.8	1.0
VEH	1156	43.577	47.841	52.699	57.417	60.402	64.276	67.704	72.806	81.379	83.760	87.829
	1157	22.541	24.244	26.663	26.416	27.836	32.604	37.543	39.683	42.385	45.447	49.241
	1167	13.740	17.308	19.122	24.041	27.752	32.169	34.671	39.244	40.032	42.338	42.005
	1168	14.518	16.549	18.925	20.198	23.178	26.958	30.427	34.342	37.685	43.847	50.184
PTH	1161	107.355	116.271	130.590	147.753	166.551	186.725	214.700	241.792	267.455	305.076	324.777
	1162	119.598	131.230	141.715	145.492	158.807	165.067	176.375	194.149	209.467	214.874	218.561
	1163	50.031	60.697	68.601	88.014	101.582	119.467	136.336	156.847	173.618	188.535	199.150
	1165	75.494	84.505	97.815	120.845	140.158	162.224	187.119	199.689	212.392	224.610	236.134
		Femurs										
		Axial position										
Spec. No.		-1.0	-0.8	-0.6	-0.4	-0.2	0.0	0.2	0.4	0.6	0.8	1.0
LOW	3	0.993	0.799	1.745	6.418	16.274	27.349	42.966	60.959	72.929	86.955	94.930
	11	10.163	14.552	19.288	21.317	26.086	45.340	61.052	80.853	95.754	116.994	152.382
	15	7.240	6.576	8.154	12.389	17.501	20.503	34.402	55.000	77.726	90.743	117.383
MED	0	29.155	44.658	60.749	95.022	128.083	147.707	176.545	223.374	256.471	277.489	301.199
	9	61.016	73.355	85.136	105.379	114.042	132.556	153.244	164.962	186.174	213.327	240.773
	24	34.355	43.299	57.193	91.572	119.957	143.759	166.214	181.649	197.651	217.901	243.418
HIGH	33	269.678	299.028	307.629	332.559	346.463	375.419	386.859	425.271	453.525	514.079	553.572
	39	147.274	178.529	195.812	234.359	276.356	304.137	322.543	363.341	396.794	435.222	474.624
	40	165.529	203.191	226.470	258.104	342.339	359.142	435.043	501.180	566.382	613.386	661.958

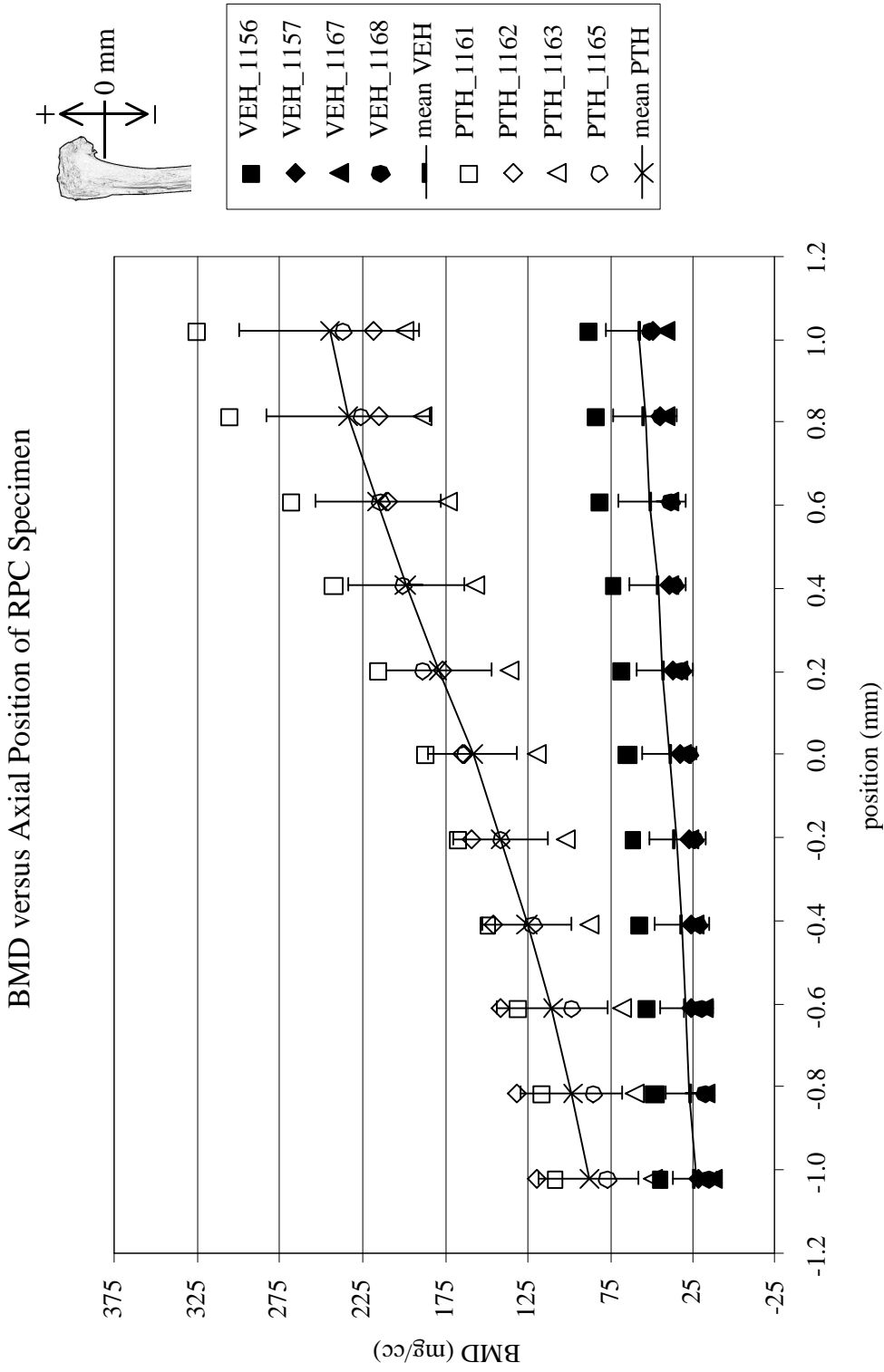


Figure 4.7. Plot of the BMD versus changes in axial position for the bones (tibias) from the HU-PTH study. Each trend line shows the mean BMD and the error bars show the 95% confidence interval on the mean BMD for each group.

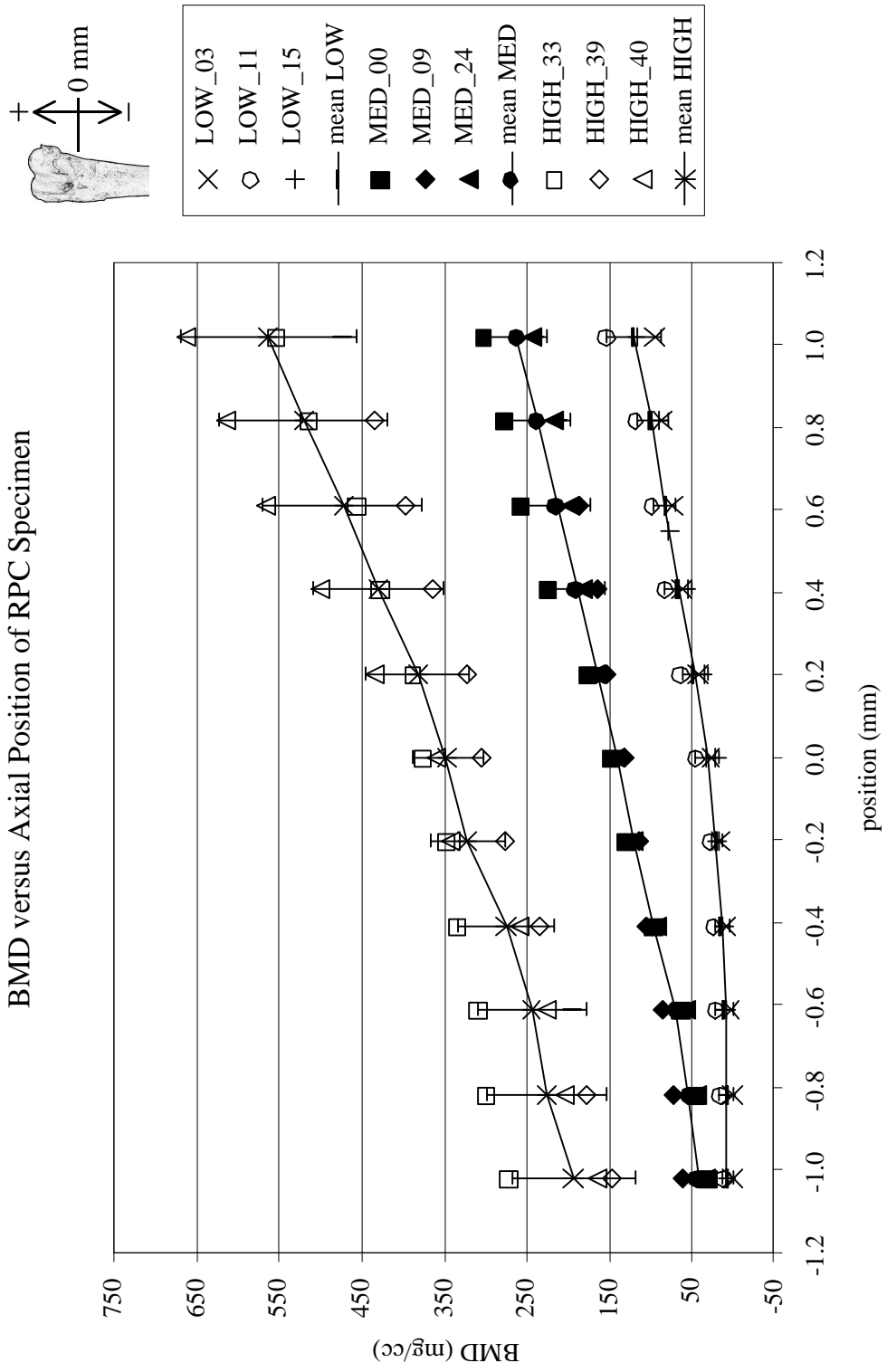


Figure 4.8. Plot of the BMD versus changes in axial position for the bones (femurs) from the OVX-IND study. Each trend line shows the mean BMD and the error bars show the 95% confidence interval on the mean BMD for each group.

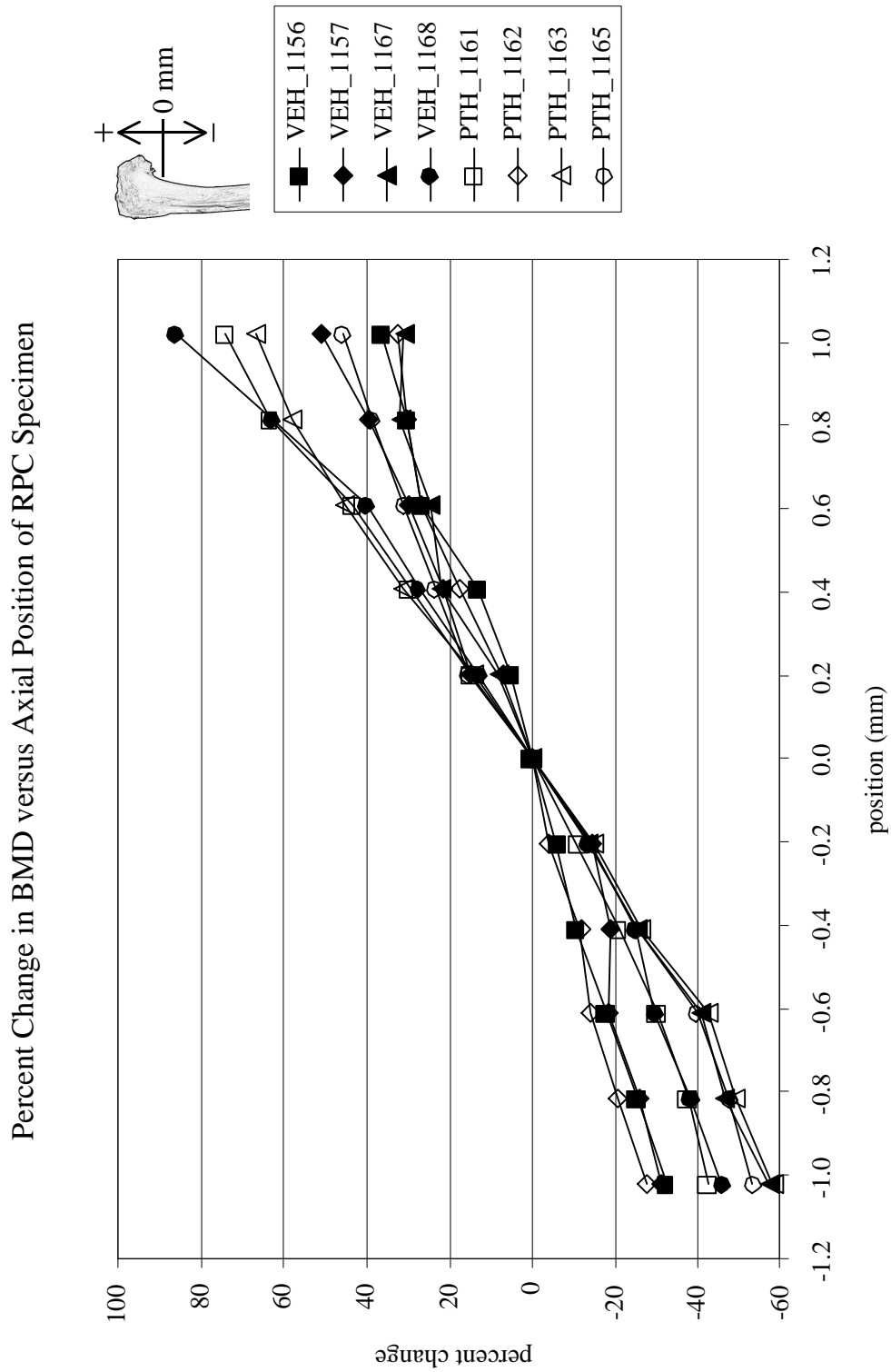


Figure 4.9. Plot of the percent change in BMD from the reference position versus axial position for the bones (tibias) from the HU-PTH study.

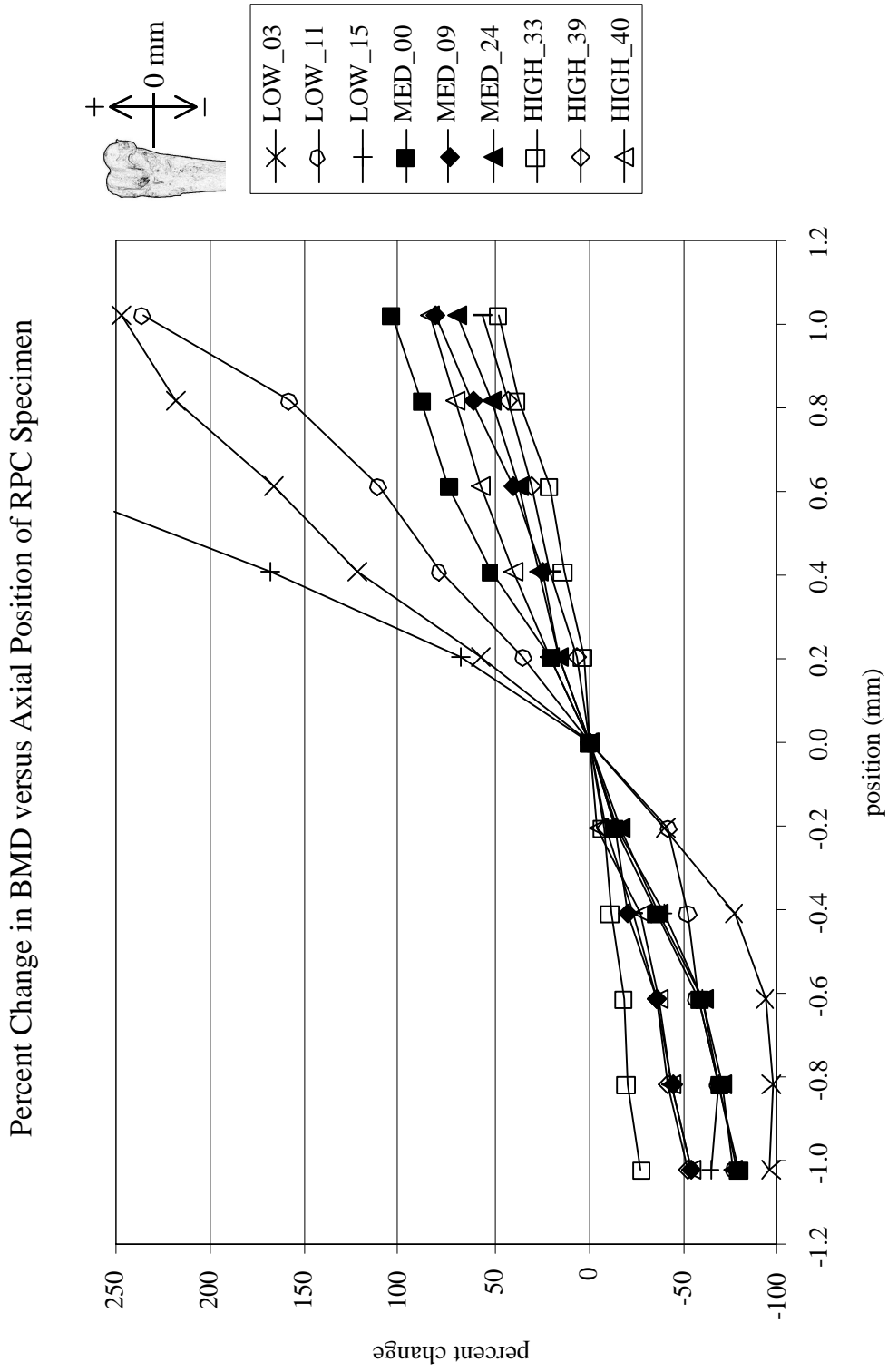


Figure 4.10. Plot of the percent change in BMD from the reference position versus axial position for the bones (femurs) from the OVX-IND study.

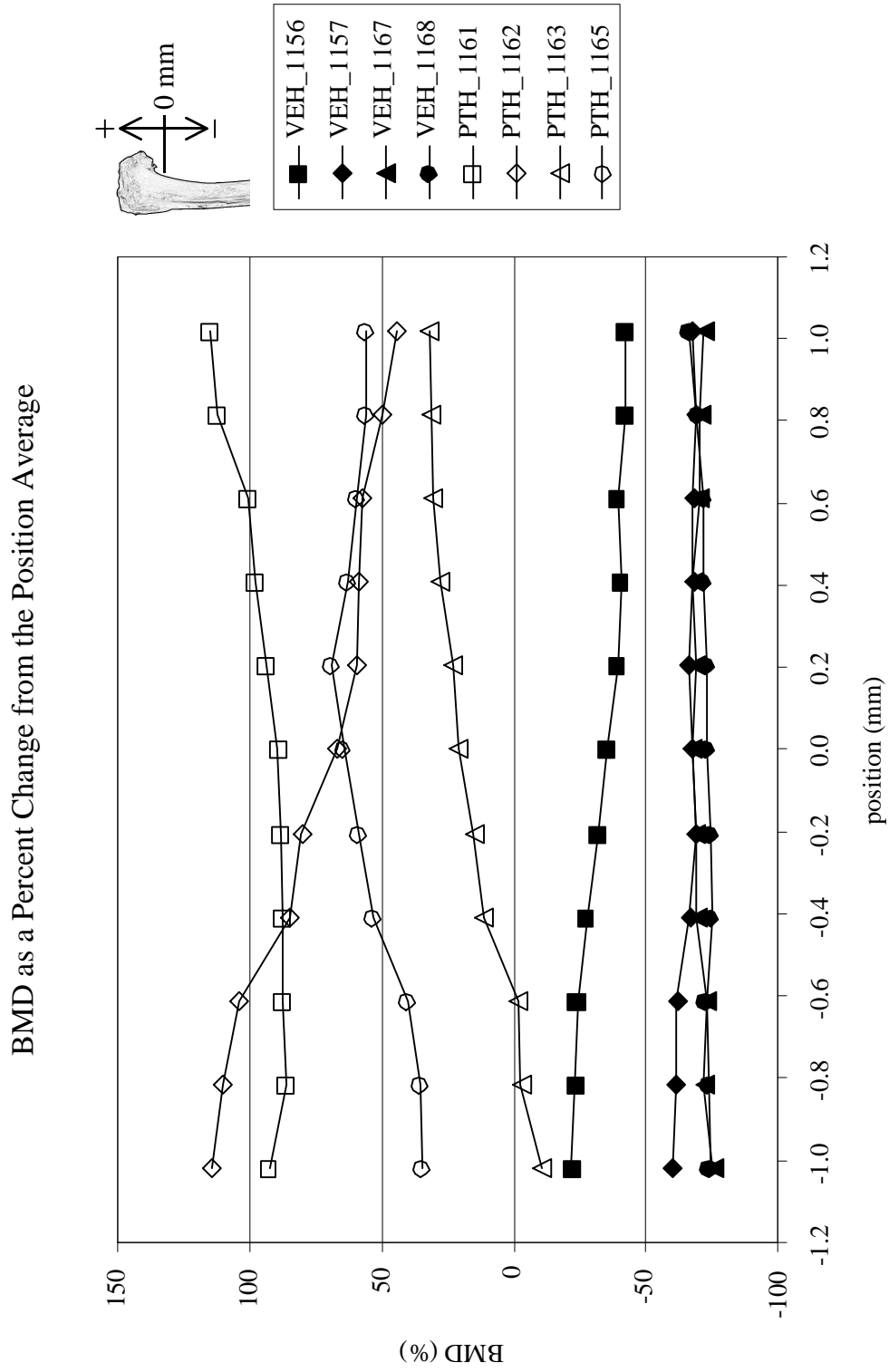


Figure 4.1.1. Plot of the percent change in BMD from the position average versus axial position for the bones (tibias) from the HU-PTH study.

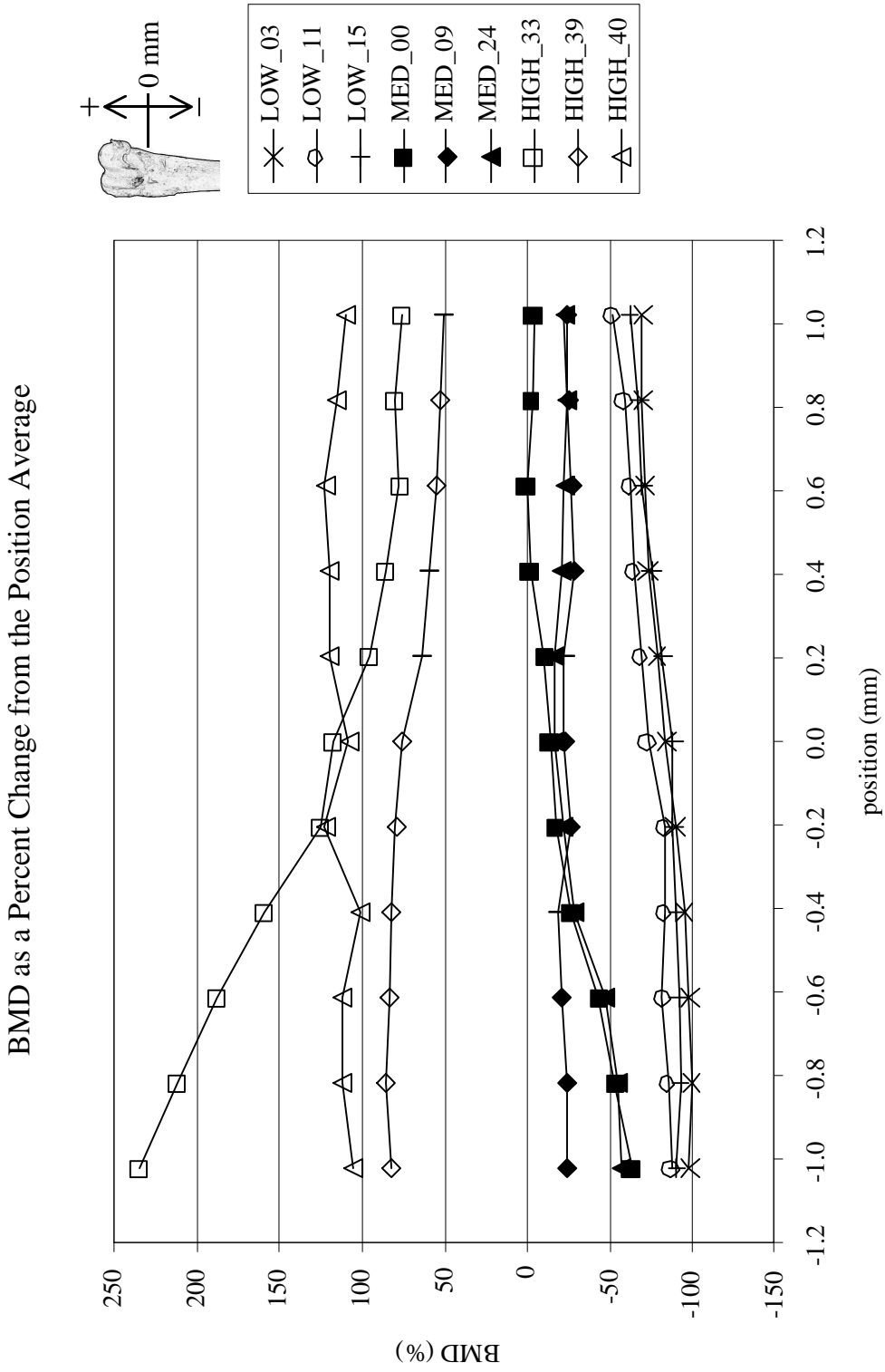


Figure 4.12. Plot of the percent change in BMD from the position average versus axial position for the bones (femurs) from the OVX-IND study.

#### 4.5. Changes in Platen Diameter

The reduction in platen diameter study shows that in all cases the BMD decreased as the diameter of the ROI is reduced. For the study, the diameter is reduced in 10% increments from 100% of the largest diameter to 10% of the diameter. Only the data from 100% to 40% is presented. Below 40%, the ROI diameter is too small and the calculated data for BMD do not appear to be correct or could not even be found. For all groups, the significance of the variation with respect to changes in the diameter from a one way ANOVA is much less than  $p=0.001$ . The p values for each group are presented in table 4.3.

Table 4.3. P values for a one way ANOVA for variation in BMD with respect to change in ROI diameter.

group	P
HIGH	7.624E-04
PTH	2.301E-08
VEH	5.688E-04
LOW	3.055E-06
MED	3.669E-15

The BMD values for the analysis of a reduction in ROI diameter are presented in table 4.4. Figure 4.13 and 4.14 show the BMD versus reduction in ROI diameter for the HU-PTH study and the OVX-IND study, respectively. On both graphs, the raw data are shown as individual points. The line with error bars shows the mean with a 95% confidence interval for each group. With both studies, the separation between confidence intervals is maintained from a 100% diameter through about a 60% diameter. At about a 50% diameter, the confidence intervals begin overlap somewhat for the OVX-IND study.

The same normalization methods used for the variation in axial position study are also used here. For the percent change in BMD, the BMD is expressed as a percent change from the 100% ROI diameter (instead of the reference position as in the axial



position study). Figures 4.15 and 4.16 show the percent change in BMD from the 100% ROI diameter for the HU-PTH study and the OVX-IND study, respectively.

Additionally, the BMD are normalized with respect to the position average using the same method as presented in the axial position study; that is the BMD are expressed as a percent change from the ROI diameter average (i.e. the average of all the BMD within a study for each percent diameter). Figures 4.17 and 4.18 show the percent change in BMD from the percent diameter for the HU-PTH study and the OVX-IND study, respectively.

Table 4.4. Bone mineral density (in mg/cc) versus the percent reduction in ROI diameter at the reference position. The bones are sorted by group. Data for reductions below 40% are not reported. These values are unreliable due to the small size of the corresponding ROI.

		Tibias						
		Percent maximum diameter						
Spec. No.		100%	90%	80%	70%	60%	50%	40%
VEH	1156	64.276	50.910	41.286	33.279	26.616	19.831	14.949
	1157	32.604	28.737	26.024	22.588	17.508	13.428	9.990
	1167	32.169	23.302	17.610	14.133	9.498	4.725	2.237
	1168	26.958	20.086	17.016	13.255	9.426	5.143	3.057
PTH	1161	186.725	168.853	153.443	142.947	133.911	118.348	100.304
	1162	165.067	154.580	148.439	137.661	119.664	112.183	101.634
	1163	119.467	101.649	88.913	80.079	67.394	53.838	42.505
	1165	162.224	151.016	143.931	135.735	117.321	87.015	62.363
		Femurs						
		Percent maximum diameter						
Spec. No.		100%	90%	80%	70%	60%	50%	40%
LOW	3	27.349	16.179	9.227	4.783	2.399	0.499	0.000
	11	45.340	26.799	18.471	8.439	4.496	1.073	0.069
	15	20.503	12.360	5.838	4.967	5.058	2.516	0.324
MED	0	147.707	109.223	85.698	59.607	35.880	29.125	17.198
	9	132.556	99.848	75.373	50.517	38.058	28.527	13.113
	24	143.759	113.180	86.379	64.068	51.490	40.728	33.247
HIGH	33	375.419	334.417	288.504	245.373	216.041	198.116	191.264
	39	304.137	250.369	190.770	141.718	83.366	40.347	20.820
	40	359.142	295.441	242.873	188.642	155.851	126.820	102.166

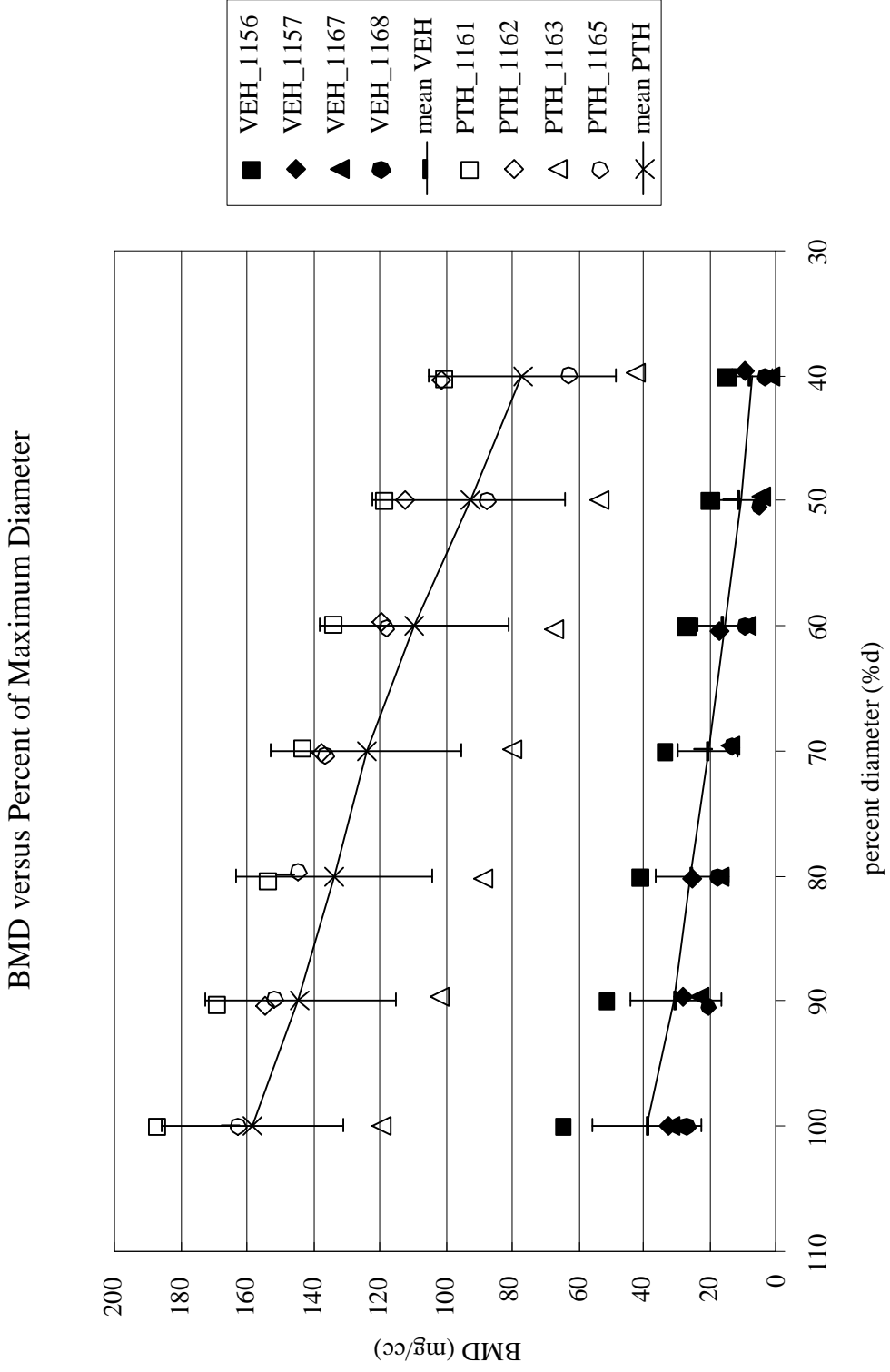


Figure 4.13. Plot of the BMD versus changes in ROI diameter for the bones (tibias) from the HU-PTH study. Each trend line shows the mean BMD and the error bars show the 95% confidence interval on the mean BMD for each group.

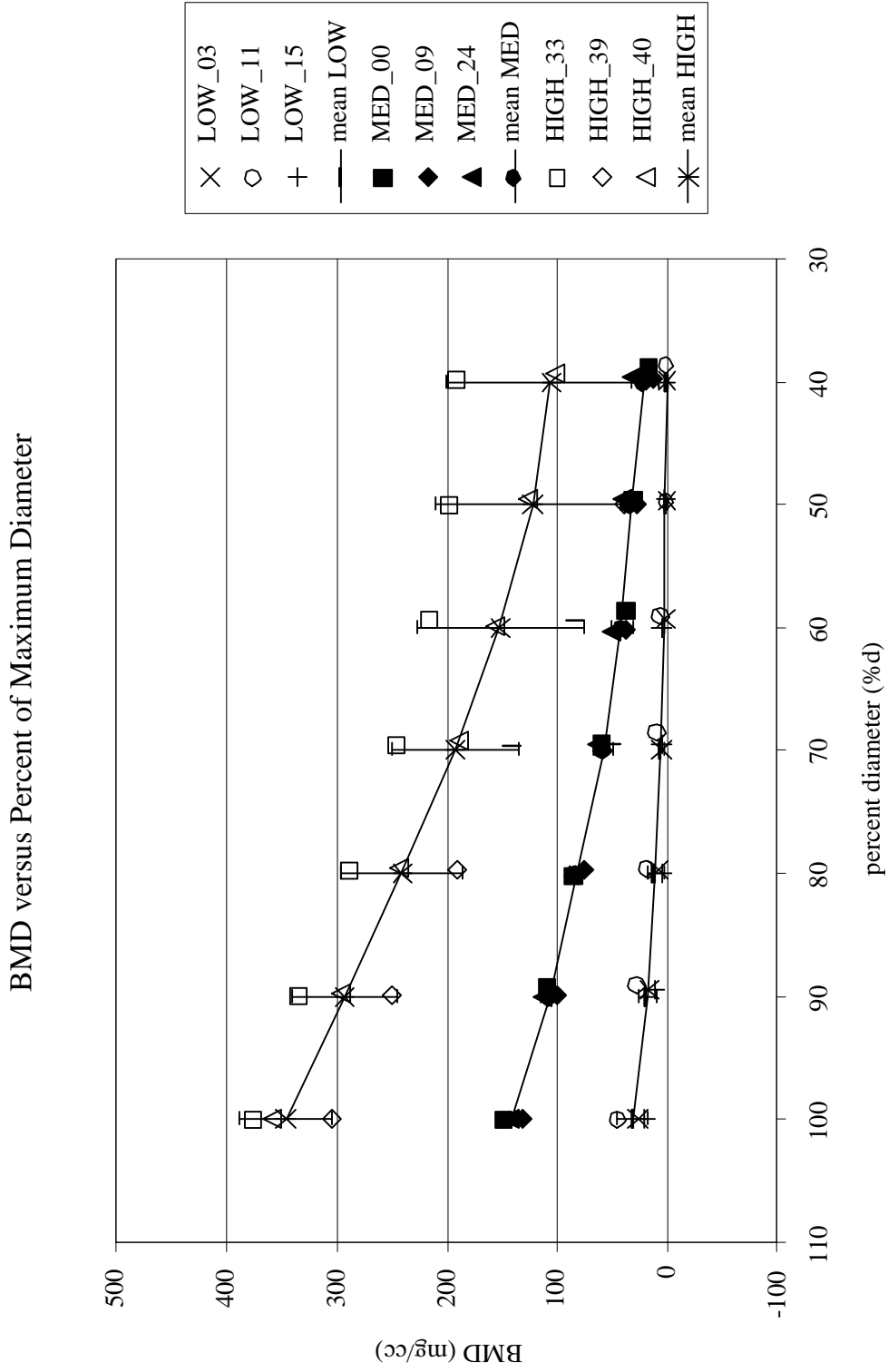


Figure 4.14. Plot of the BMD versus changes in ROI diameter for the bones (femurs) from the OVX-IND study. Each trend line shows the mean BMD and the error bars show the 95% confidence interval on the mean BMD for each group.

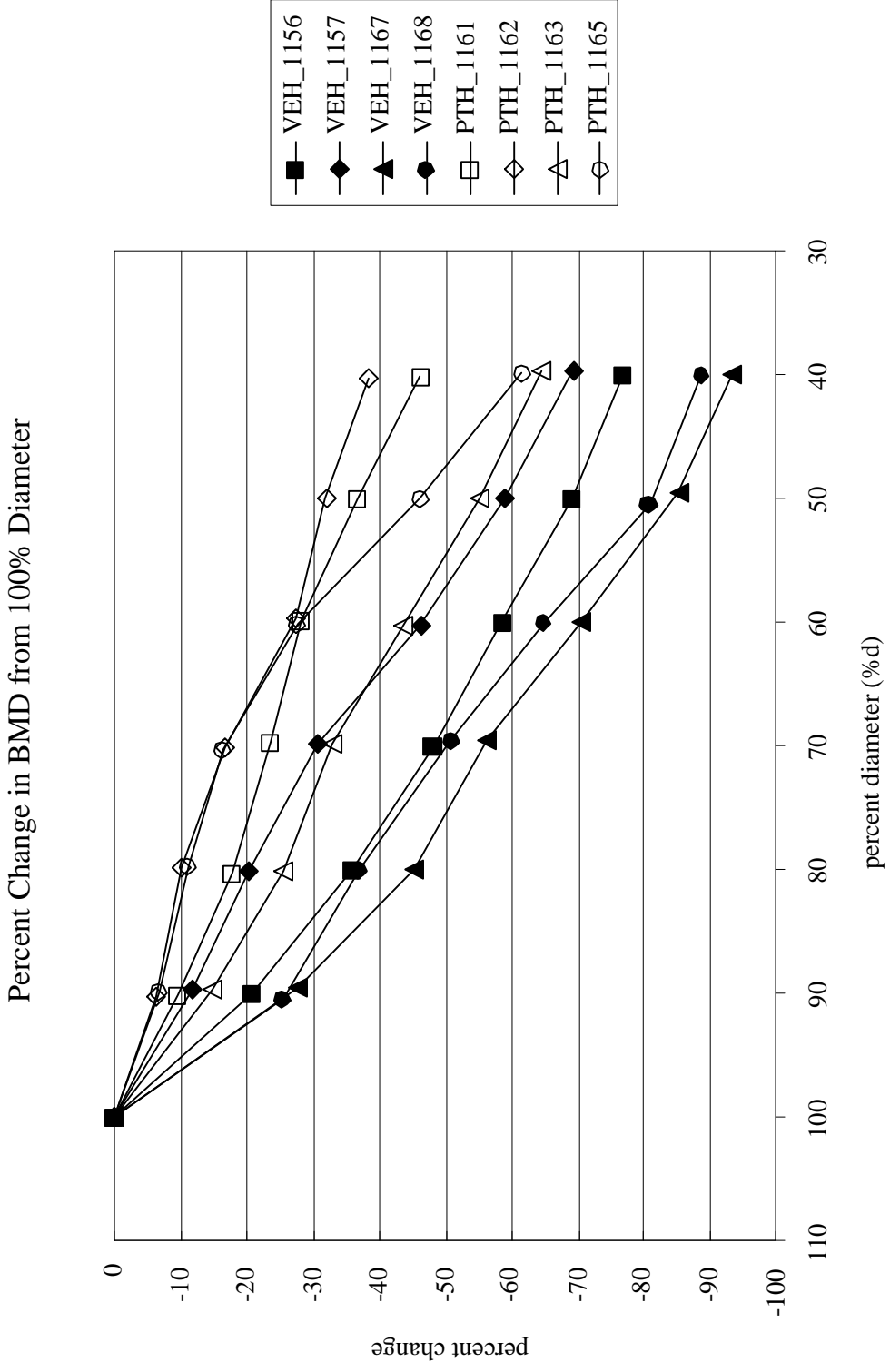


Figure 4.15. Plot of the percent change in BMD from the 100% ROI diameter for the bones (tibias) from the HU-PTH study.

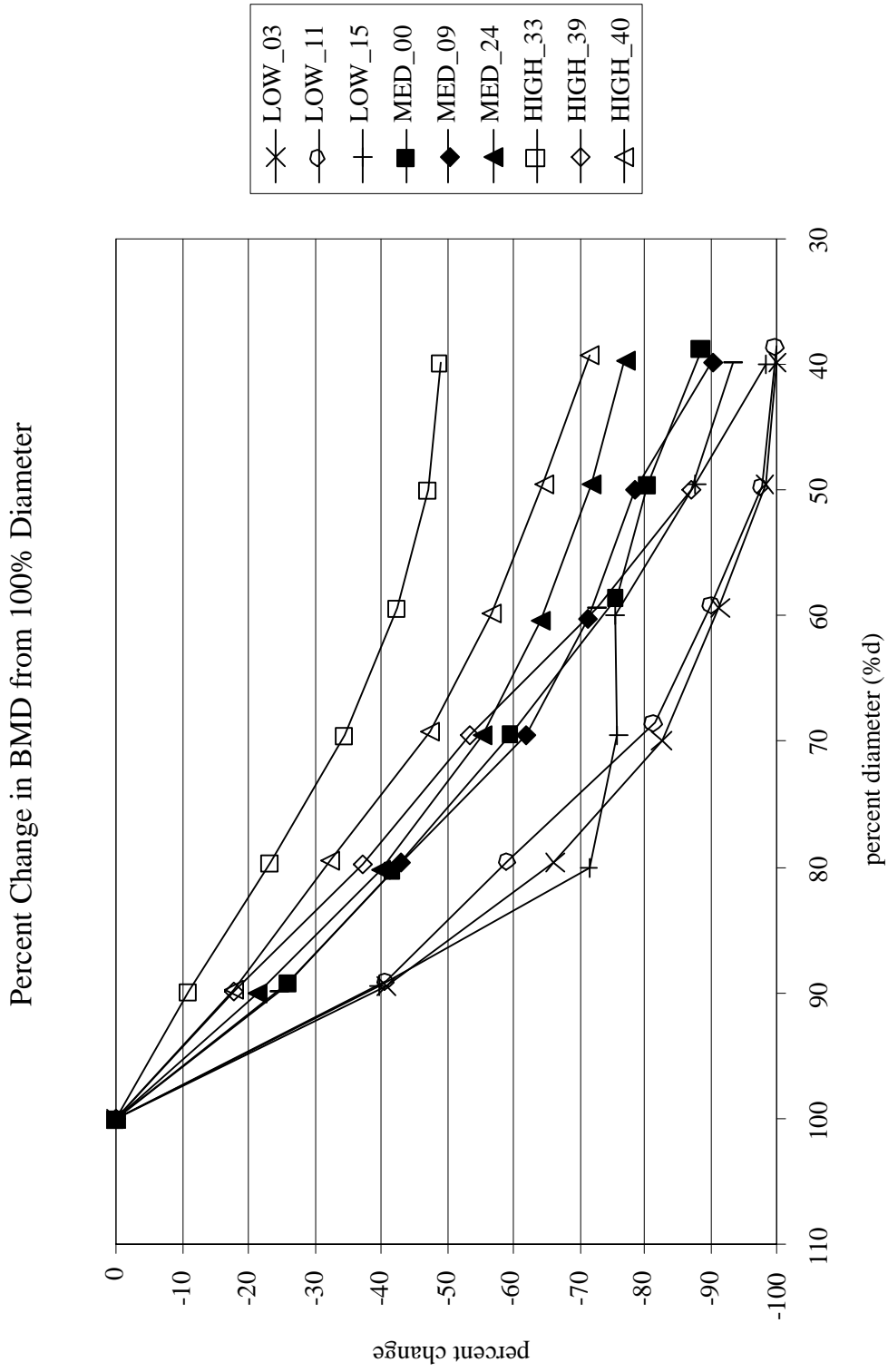


Figure 4.16. Plot of the percent change in BMD from the 100% ROI diameter for the bones (femurs) from the OVX-IND study.

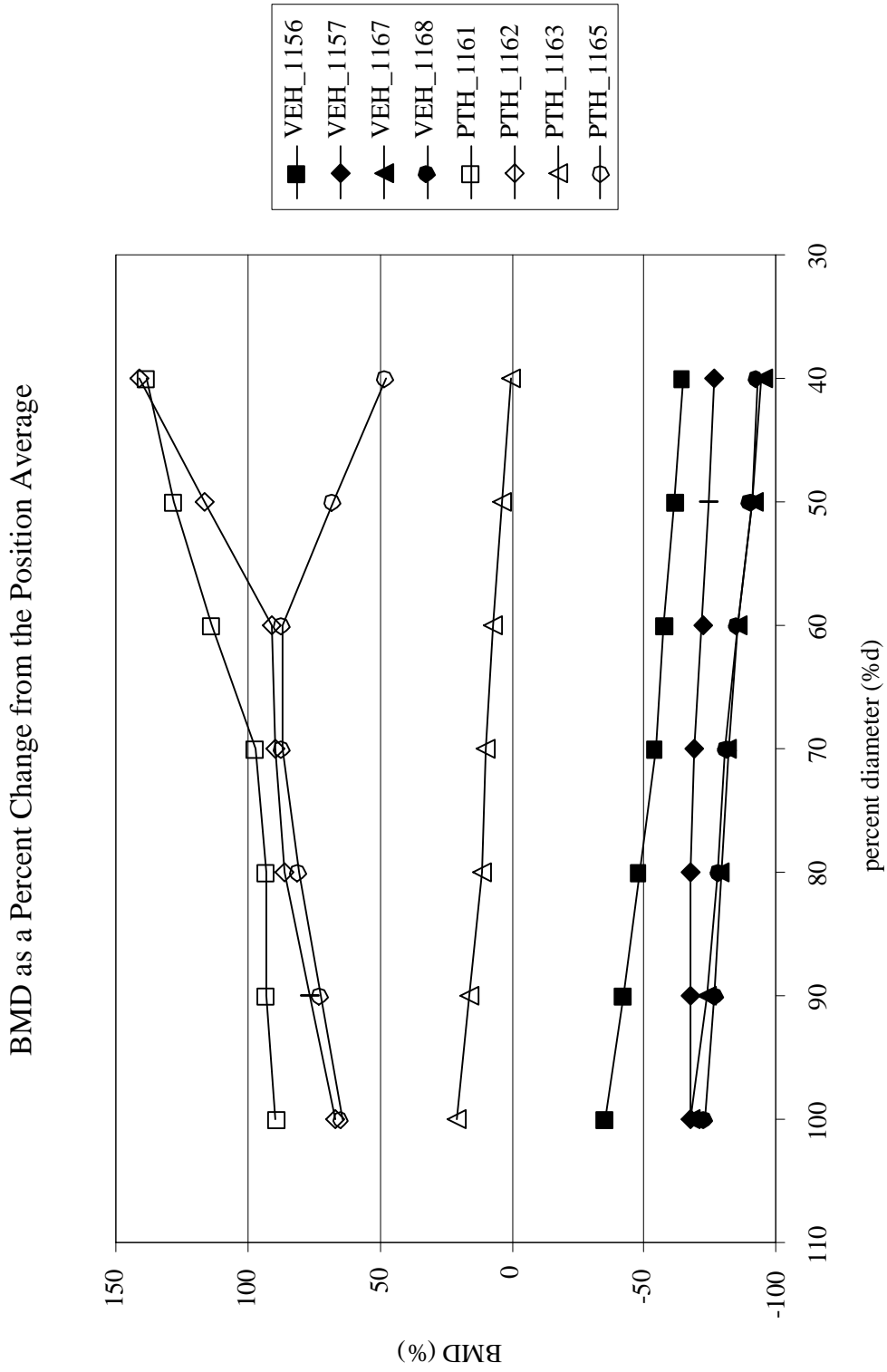


Figure 4.17. Plot of the percent change in BMD from the percent diameter average for the bones (tibias) from the HU-PTH study.

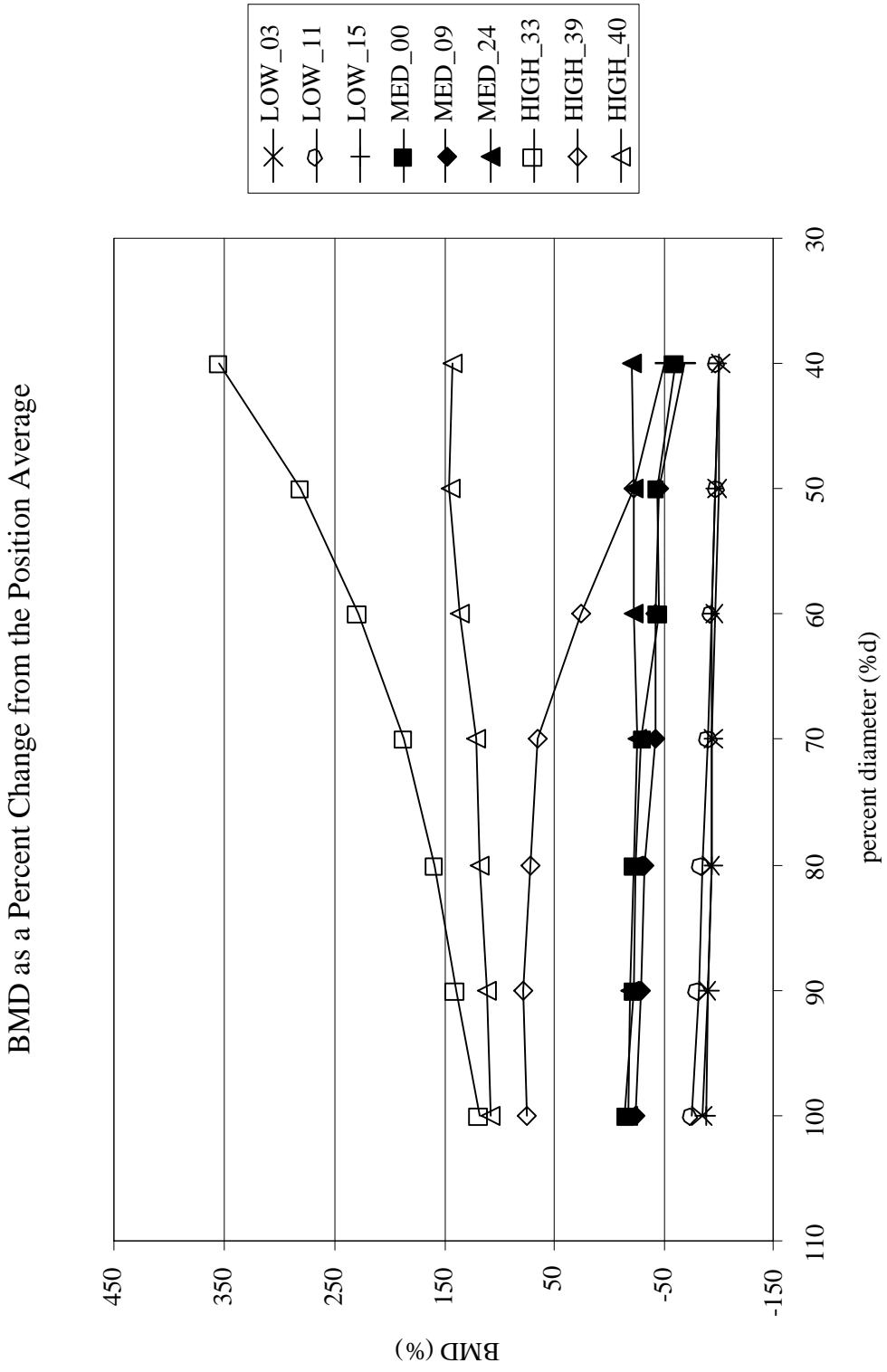


Figure 4.18. Plot of the percent change in BMD from the percent diameter average for the bones (femurs) from the OVX-IND study.



## 5. DISCUSSION

### *5.1. New Specimen Location Method*

Using external landmarks instead of contact radiographs to locate the RPC specimen satisfactorily fulfills the objectives of this research work. These main objectives are to decrease the amount of time required to obtain an RPC specimen and to improve the quality of the results obtained from the RPC test.

Using external landmarks to identify the target RPC specimen location has several advantages over using contact radiographs to determine the specimen location. The obvious advantage is time. Obtaining, digitizing and analyzing contact radiographs to determine the RPC specimen location requires a significant amount of time. By using external landmarks, the specimens can be cut from the bone without any prior analysis or preparation.

Another advantage of using external landmarks to locate the RPC specimen is a higher level of consistency. The landmarks are the same on all bones and clearly show the furthest extent of the growth plate. This results in less uncertainty when compared to using contact radiographs. With contact radiographs, the actual location of the desired RPC specimen is difficult to determine due to difficulty in identifying the growth plate and due to radiographic decay. With the contact radiographs, it is not always clear where the precise location of the growth plate is. Often, the location has to be estimated as best possible.

### *5.2. Position*

When looking at the BMD data for changes in axial position, there does not appear to be any “ideal” cutting location. As expected, the BMD increases as the RPC specimen location approaches the growth plate and decreases as the location moves away from the growth plate. Around the reference position, this change is fairly linear with no flat regions or any other features that would indicate one location being better

than another. For all groups, except the VEH group from the HU-PTH study, the BMD did significantly vary with the axial position ( $P < 0.00001$ ).

The fact that the VEH group did not significantly vary with the axial position does seem unusual. The lack of significant variation is likely due to the amount of bone lost during hindlimb unloading. The BMD probably did not vary because there was not that much bone there to begin with and the bone was lost from the entire metaphysis.

### *5.2.1. BMD versus Position*

The two plots showing BMD versus the axial position of the RPC specimen (figures 4.7 and 4.8, pp. 33-34) show how the BMD varies with position. Two significant observations can be made from these two graphs.

First, for most of the axial positions (except maybe those farthest away from the growth plate, i.e. an axial position approaching  $-1$  mm) there remains a significant gap between all of the groups within each study. For the OVX-IND study, these gaps remain fairly constant. The gap for the HU-PTH study decreases as the RPC location moves away from the growth plate, yet the gap does remain significant across the whole range.

Second, if the RPC specimens from a low BMD group are cut too close to the growth plate and specimens from a medium or high BMD group are cut too far away from the growth plate, it is possible that the significance between the two groups could be lost. This would be detrimental to the results of a study as the data would show no significant difference when one really exists. A similar problem would occur with two groups that do not have a significant difference if one group is cut too close to the growth plate and the other too far away. The result would be a significant difference that does not really exist. This indicates that cutting the RPC specimen consistently from the same spot is essential.

### *5.2.2. Percent Change in BMD from Reference Position*

One method used to normalize the BMD values for changes in axial position is to express the BMD as a percent change from the reference RPC position. This

normalization is shown in two plots (figures 4.9 and 4.10, pp. 35-36). All groups, except for the HIGH group from the OVX-IND study, show a fairly linear variance with respect to the change in position. Again, the discrepancy in the high BMD group can likely be attributed to irregularities in animal studies. It is also possible that upon approaching the growth plate the ROI contains significant amounts of growth plate, which could also lead to the large increase in percent change in BMD. The most significant observation from these two graphs is that the percent change at each position is basically the same for all groups within each study. There is also no clear separation between groups at each position indicating that no one RPC location is better than another.

### *5.2.3. BMD as a Percent of Position Average*

A second method used to normalize the BMD versus axial position data is expressing the BMD as a percent change from the position average. The two graphs (figures 4.11 and 4.12, pp. 37-38) representing this data show most of the bones maintain a fairly constant ranking across the whole range of positions investigated. The exceptions can again be attributed to animal irregularities. It should also be noted that while the bones retain their percent change from the position average, the difference between the groups remains evident.

### *5.3. Diameter*

The decrease in BMD with respect to the reduction in diameter (figure 4.13 and 4.14, pp. 42-43) is expected. There is a higher concentration of trabeculae near the cortical wall of long bones. The concentration of trabeculae decreases towards the center of the cancellous core. Other researchers have confirmed this result (Oxlund et al., 2002). This is also demonstrated by looking at contact radiographs of cut RPC specimens used for platen sizing. The x-rays consistently are darker in the center of the cancellous cavity and get lighter on approaching the cortical wall. The darker region indicates that there is less bone material present and hence a lower BMD.

These findings suggest that the largest size platen possible should be used when performing the RPC test. A larger platen size will test more of the cancellous bone and will give a better estimation of the true mechanical properties. Additionally, RPC specimens often have large holes or cavities. If the platens are not large enough, they will not be able to test what cancellous bone is present.

Unfortunately, using a larger platen size can be difficult to achieve in practice. The actual RPC specimens are small and the largest possible platen diameter is almost always less than 3 mm. Ensuring that the platen does not compress the cortical wall of the test specimen must also be considered; otherwise, the test results would contain significant errors. In addition, finite element modeling of the RPC test suggests that experimental artifact increases as the platen size approaches 100% of the largest possible platen size. Even though direct contact with cortical bone is avoided, the cortical bone carries more of the compressive load as the platen size increases (Rogers, 2002). Hence, choosing the platen size becomes a tradeoff between achieving the largest platen diameter possible and avoiding the risk of compressing cortical bone during the test. Current procedures use hand positioning and no vision enhancements (e.g. magnifying glass or digital video camera) to position the RPC specimen for testing. This makes using a large platen size even more difficult.

### *5.3.1. Percent Change in BMD from 100% Diameter*

One method used to normalize the BMD values for changes in platen size is to express the BMD as a percent change from the 100% ROI diameter. This normalization is shown in two plots (figures 4.15 and 4.16, pp. 44-45). All groups show a fairly linear variance with respect to the change in position from 100% through 70%. After 70%, a linear variation is not maintained. The most significant observation from these two graphs is that the span of the percent change is tighter near a 100% diameter.

### 5.3.2. *BMD as a Percent of Percent Diameter Average*

A second method used to normalize the BMD versus platen size data is expressing the BMD as a percent change from the percent diameter. The two graphs (figures 4.17 and 4.18, pp. 46-47) representing this data show most of the bones maintain a fairly constant ranking from 100% through around 70%. Below 70%, the rankings change dramatically. It should also be noted that while the bones retain their percent change from the position average, the difference between the groups remains evident.

## 6. CONCLUSIONS AND RECOMMENDATIONS

### *6.1. New RPC Specimen Preparation Procedure*

Locating the top plane of the desired RPC specimen for the distal rat femur and proximal rat tibia using the most proximal point of the patellar surface and the tibial tuberosity, respectively, is recommended. The presented analysis shows that, from a BMD perspective, any location around the identified landmarks will provide an adequate RPC specimen location. Because of this, knowledge gained from comparing external landmarks of the bone anatomy with growth plate topography justifies the use of the specified landmarks as the top of the RPC specimen.

Bone anatomy and growth plate topography show that the previously identified RPC specimen location is a good location. It is just barely beyond the growth plate, providing a specimen that should still contain sufficient cancellous material for the RPC without having any growth plate. There may still be a small amount of primary spongiosa near the cortical wall by the specified landmarks, but the amount is small. Since this primary spongiosa is located near the cortical wall on the end of the specimen that has the larger diameter, it should not affect the results.

### *6.2. Analysis of Variations in RPC Specimen Position and Platen Size*

The study of variation in RPC specimen location indicates that there is no one ideal location for the actual RPC specimen. It does, however, show that the specified external landmarks are sufficient choices. The study also shows that, whichever point is used, the critical factor is consistency. This calls for an addition to the specimen preparation procedures. Each person that cuts RPC specimens will likely tend to bias his or her cut to one side or the other of the specified landmark. This is acceptable so long as the cuts are always biased in the same direction and by the same amount. A problem could arise if several different people are cutting bones for the same study. If one person tends to cut closer to the growth plate and another tends to cut away from the growth plate, the

difference due to axial variation may be large enough that the significance of a particular comparison could be lost. Hence, the recommendation of having only one person cut all bones within a particular study is made.

As can be seen from the reduction in diameter study, the BMD drops significantly with reductions in diameter. Using a 70% diameter for the ROI can cause as much as a 44% reduction in BMD (HIGH group from OVX-IND study). Clearly, using the largest platen diameter possible for the RPC test is desirable. Using a platen reduction of 80% should be achievable without any other modifications to the test procedures. It mostly requires more patience and greater care when positioning the RPC specimen on the platens. In the case of the HIGH group, using an 80% reduction in diameter would change the percent loss in BMD from 44% to 30%. This is a significant gain compared to the change in platen size.

Additionally, the normalization indicates that for platen reductions below 70%, the bones do not hold their standing in relation to the other bones and reduction below 70% should be avoided. However, this recommendation should also take into account the issue of potentially higher load sharing by the cortical shell with larger platen sizes as well as the risk of compressing cortical bone during the test.

### *6.3. Limitations of Results*

The findings of this work need to take into consideration the fact that they are based on BMD alone. The RPC test is used to find mechanical properties such as ultimate stress, modulus of elasticity, etc. While BMD does correlate with mechanical properties, it is not a perfect predictor and does not always show the true mechanical properties.

### *6.4. Recommendations for Future Work*

During this work, several opportunities for improvements and or investigations on the RPC test have become apparent. Several of these possibilities are discussed below.

#### *6.4.1. Finite Element Analysis*

Micro-CT scans can be used to generate a finite element mesh that corresponds to the actual bone geometry (Ito et al., 2002). There are a lot of unanswered questions that could be explored using finite element analysis. For example, one issue that has not been addressed is the effect of misalignment of the RPC specimen when being tested. This undoubtedly introduces a source of error in the experimental results, but the magnitude of this error is not known.

It would also be beneficial to duplicate the work done in this thesis using finite element analysis. Finite element analysis more closely represents the RPC test than a BMD analysis does since the cancellous structure is analyzed. Other researchers have found only a weak correlation between BMD and mechanical properties for sites containing mostly cancellous bone and have recommended the use of finite element models developed from micro-CT scans as a better alternative (Stenstrom et al., 2000)

#### *6.4.2. Rapid Prototyping*

The isosurface-rendering tool in MicroView has the capability of producing a stereolithography file that can be used to make a rapid prototype. These stereolithography files can be made from a defined ROI allowing models to be made of a desired RPC specimen including cancellous architecture. These “copies” of the RPC specimen could then be mechanically tested using the RPC test.

A few rapid prototypes have been made using a rapid prototype machine available in the Texas A&M Mechanical Engineering Department. There are many issues that still need to be worked out before using rapid prototypes to assess the effect of varying the RPC specimen location, but its use could provide valuable insight that is lost when looking at BMD alone.

#### *6.4.3. Improved Cutting Methods*

Current RPC specimen preparation procedures use an Isomet low speed diamond wafering saw to cut the specimen from the bone. The difficulty arises in aligning the



bone with the saw blade. The bone is positioned above the saw making it difficult to accurately align the bone landmark with the saw blade. Some form of vision enhancement would significantly decrease this difficulty and improve the alignment accuracy.

#### *6.4.4. Improved RPC Positioning*

An endocortical circle diameter reduction of 70% is currently used for determining the platen size, primarily due to the difficulty of centering each specimen in the materials testing machine. The specimen is positioned by hand without any form of vision enhancement. The problem arises in trying to use a larger platen size while ensuring that only cancellous bone is being tested. The use of vision enhancement, either in the form of a magnifying glass or a high-resolution digital video camera connected to a computer, as well as some form of specimen positioning apparatus, would allow the use of a larger platen size.

## REFERENCES

- Bauss, F., Lalla, R.E., Hothorn, L.A., 2002. Effects of Treatment with Ibandronate on Bone Mass, Architecture, Biomechanical Properties, and Bone Concentration of Ibandronate in Ovariectomized Aged Rats. *The Journal of Rheumatology* 29, 2200-2208.
- Chachra, D., Lee, M.L., Kasra, M., Grynepas, M.D., 2000. Differential Effects of Ovariectomy on the Mechanical Properties of Cortical and Cancellous Bone in Rat Femora and Vertebrae. *Biomedical Sciences Instrumentation* 36, 123-128.
- Ito, M., Nishida, A., Koga, A., Ikeda, S., Shiraishi, A., Uetani, M., Hayashi, K., Nakamura, T., 2002. Contribution of Trabecular and Cortical Components to the Mechanical Properties of Bone and Their Regulating Parameters. *Bone* 31, 354-358.
- Ke, H.Z., Shen, V.W., Qi, H., Crawford, D.T., Wu, D.D., Liang, X.G., Chidsey-Frink, K.L., Pirie, C.M., Simmons, H.A., Thompson, D.D., 1998. Prostaglandin E<sub>2</sub> Increases Bone Strength in Intact Rats and in Ovariectomized Rats with Established Osteopenia. *Bone* 23, 249-255.
- Kimmel, D.B., 1991. Quantitative Histologic Changes in the Proximal Tibial Growth Cartilage of Aged Female Rats. In: Jee, W.S.S. (Ed.), *The Aged Rat Model for Bone Biology Studies: Cells and Materials Supplement 1. Scanning Microscopy International*, Chicago, pp. 11-18.
- McLean, F.C., Urist, M.R., 1968. *Bone, Fundamentals of the Physiology of Skeletal Tissue*, 3rd Edition. The University of Chicago Press, Chicago.
- Montgomery, D.C., 2001. *Design and Analysis of Experiments*, 5th Edition. John Wiley and Sons, Inc., New York.
- Mosekilde, L., Thomsen, J.S., Orhii, P.B., Kalu, D.N., 1998. Growth Hormone Increases Vertebral and Femoral Bone Strength in Osteopenic, Ovariectomized, Aged Rats in a Dose-Dependent and Site-Specific Manner. *Bone* 23, 343-352.
- Nguyen, L., 2001. Estimating Changes in the Mechanical Properties of the Femur in the Adult and Aged Rat due to Adult-Onset Alcohol Consumption. Masters Thesis, Texas A&M University, College Station, TX.
- Ogden, J.A., 1980. Chondro-Osseous Development and Growth. In: M.R. Urist (Ed.), *Fundamental and Clinical Bone Physiology*. J.B. Lippincott Company, Philadelphia, pp. 108-171.
- Oxlund, H., Dalstra, M., Ejersted, C., Andreassen, T.T., 2002. Parathyroid Hormone Induces Formation of new Cancellous Bone with Substantial Mechanical Strength at a Site where it had Disappeared in Old Rats. *European Journal of Endocrinology* 146, 431-438.

- Rogers, W., 2002. Methods and Modeling for the Reduced Platen Compression of Cancellous Bone in the Rodent Proximal Tibia. Masters Thesis, Texas A&M University, College Station, TX.
- Ruhmann, S., 1998. Methods for Testing the Strength of Cancellous Bone and Testing Method Effects on Cortical Bone in the Ovariectomized Rat. Masters Thesis, Texas A&M University, College Station, TX.
- Siegel, I.M., 1998. All About Bone, an Owner's Manual. Demos Medical Publishing, Inc., New York.
- Stenstrom, M., Olander, B., Lehto-Axtelius, D., Madsen, J.E., Nordsletten, L., Carlsson, G.A., 2000. Bone Mineral Density and Bone Structure Parameters as Predictors of Bone Strength: An Analysis Using Computerized Microtomography and Gastectomy-Induced Osteopenia in the Rat. *Journal of Biomechanics* 33, 289-297.
- Vico, L., Bourrin, S., Novikov, V., Very, J.M., Chappard, D., Alexandre, C., 1991. Adaptation of Bone Cellular Activities to Tail Suspension in Rats. In: Jee, W.S.S. (Ed.), *The Aged Rat Model for Bone Biology Studies: Cells and Materials Supplement 1*. Scanning Microscopy International, Chicago, pp. 143-150.
- White, T.D., 2000. *Human Osteology*, 2nd Edition. Academic Press, San Diego.

## VITA

Heber Lemmon was born in Idaho Falls, Idaho in 1976. He moved to Moscow, Idaho when he was 10 and there graduated from Moscow High School in 1995. Heber received a Bachelor of Science from the University of Idaho in Moscow in May of 2001. He then went to Texas A&M University where he earned his Master of Science in Mechanical Engineering in August of 2003. After earning his Master of Science, he began work at Lockheed Martin in Fort Worth, Texas working on the Joint Strike Fighter Wing Box Team. He can be contacted at:

Heber Lemmon  
3300 Riveroad Ct. #1304  
Fort Worth, TX 76116